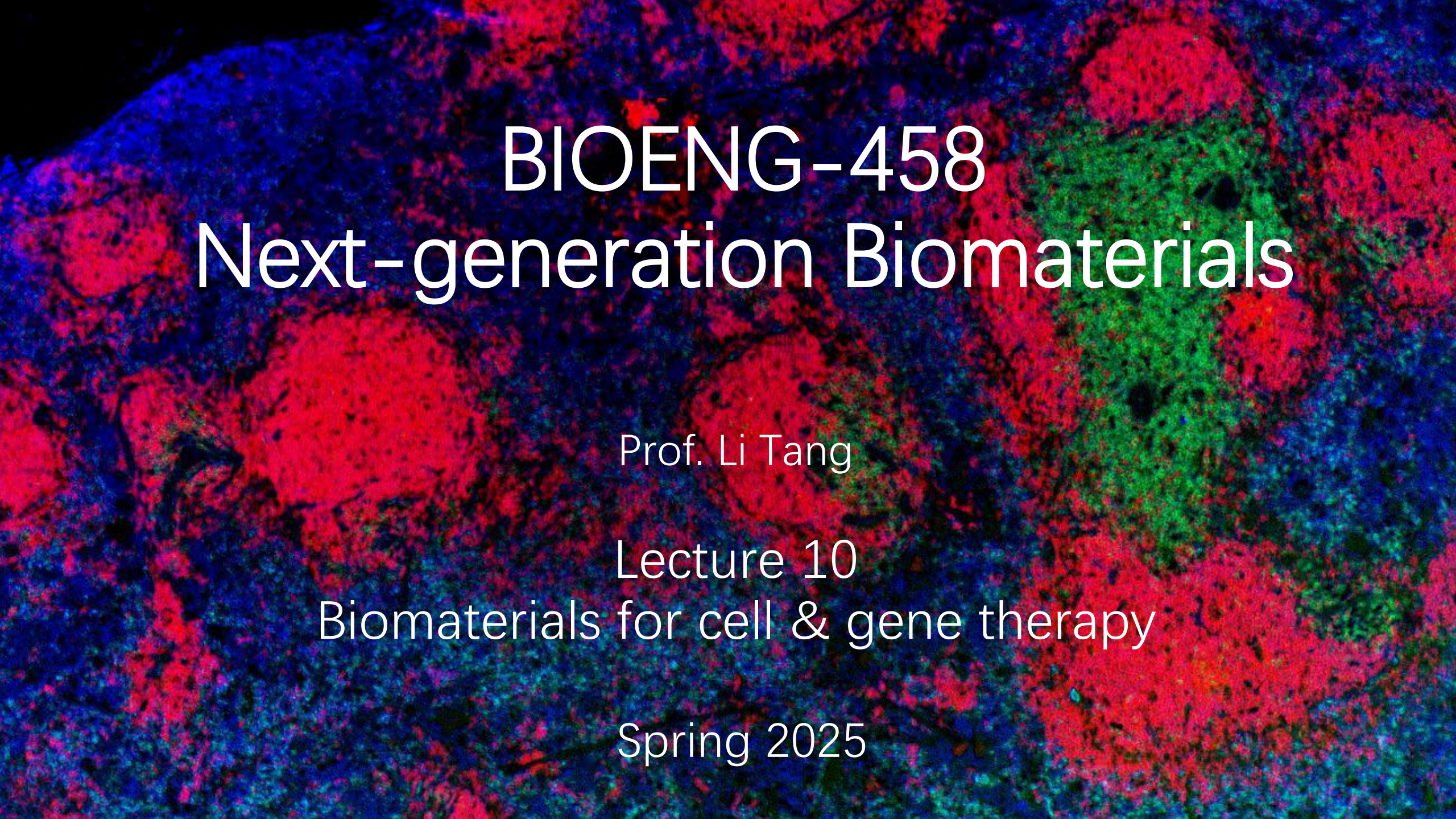

BIOENG-458
Next-generation Biomaterials

Prof. Li Tang

Lecture 10
Biomaterials for cell & gene therapy

Spring 2025

Cell and Gene Therapy (CGT) is one of the most promising new frontiers in advanced therapies for various diseases.

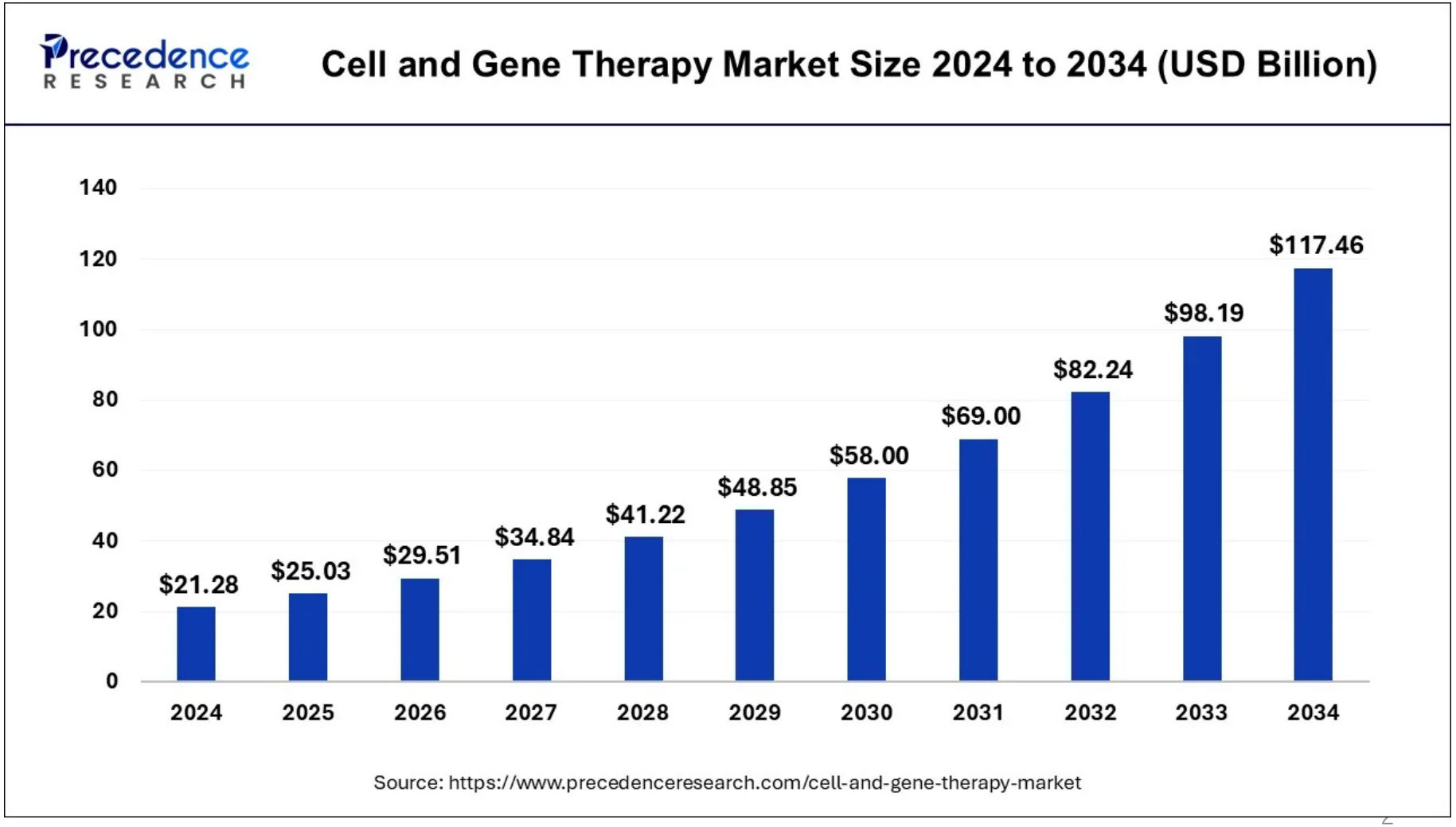

https://www.precedenceresearch.com/insightimg/cell-and-gene-therapy-market-size.webp

Definition – what is Cell&Gene Therapy (CGT)

- **Cell Therapy**: The use of living cells (e.g., stem cells, immune cells) to repair, replace, or regenerate damaged tissues. Examples include CAR-T cells for cancer and encapsulated pancreatic islets for diabetes.

- **Gene Therapy**: Modification of genetic material to treat disease, including gene replacement (e.g., Luxturna® for inherited blindness), gene silencing (e.g., siRNA), and gene editing (e.g., CRISPR/Cas9)

Gene therapy research assesses three main approaches

(i) **introduce exogenous genes into diseased cells** to produce normal gene expression products to further supplement missing or loss-of-function proteins (i.e., by upregulating gene expression);
(ii) **downregulating gene expression** by using small interfering RNA (siRNA), antisense oligonucleotides (ASOs), short hairpin RNA (shRNA), or microRNA (miRNA);
(iii) **editing mutated genes** using zinc finger nucleases, transcription activator-like effector nucleases, or CRISPR/Cas9 technology, resulting in gain or loss-of-function.

CGTs can be grouped into three broad types of technologies

- ❑ cell and gene-modified cell therapies
- ❑ gene therapy and genome editing
- ❑ DNA and RNA therapeutics

Therapy Type	Description	Key Therapeutic Areas Addressed	Example Product
Cell and Gene-Modified Cell Therapies	Restoring or genetically modifying certain sets of cells, or by using cells to carry a therapy through the body (including CAR-T)	Oncology	Kymriah
Gene Therapy & Genome Editing	Replacing, inactivating, or introducing genes into cells or modifying genome sequences (e.g., AAV gene therapies)	CNS, Ophthalmology, Rare Diseases	Luxturna
DNA & RNA Therapeutics	Treating diseases by leveraging cellular mechanism to turn off or modify gene expression (e.g., RNA interference)	CNS, GI / liver disease	Onpattro

Source: Kx research and analysis

[Cell and Gene Therapy: The Next Frontier in Healthcare]

Commercial examples

•**Cell Therapy**: Kymriah®, Yescarta® (CAR-T for blood cancers)

The first CGT was approved by the FDA in 2017 (Kymriah – developed by Novartis and indicated for acute lymphoblastic leukemia and diffuse large B-cell lymphoma)

•**Gene Therapy**: Luxturna® (AAV for retinal dystrophy), Zolgensma® (AAV for SMA).

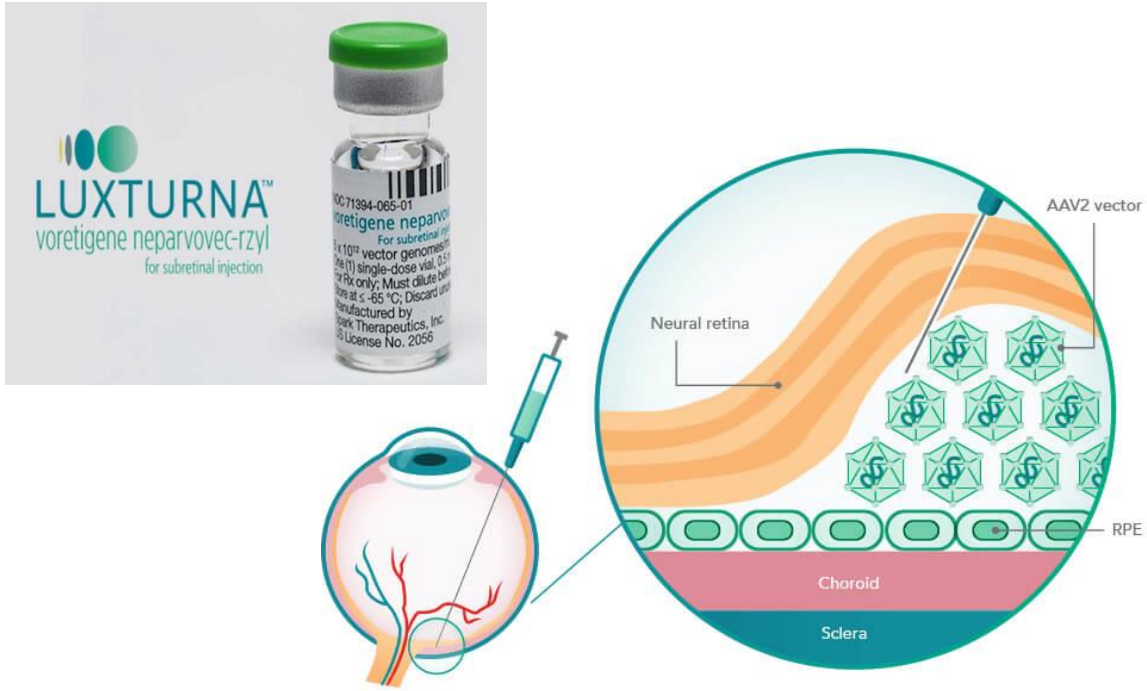

Luxturna, approved by the FDA in 2017, can restore vision in children and young adults with a rare disease that would otherwise lead to blindness.

FDA Approved and Marketed CGTs (2017-2021)

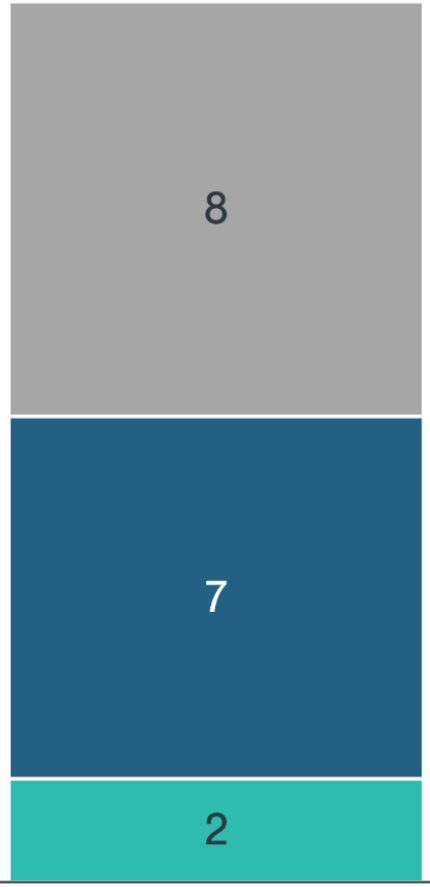

DNA & RNA Therapeutics

onpattro (patisiran) lipid complex injection

LEQVIO (inclisiran) injection 284 mg/1.5 mL

Tegsedi (inotersen) injection 284 mg/1.5 mL

VYONDYS 53 (golodirsen) Injection

GIVLAARI (givosiran) injection for subcutaneous use 189 mg/mL

OXLUMO (lumasiran) for injection 94.5 mg/0.5 mL

Viltepso (viltolarsen) injection

AMONDYS 45 (casimersen) Injection

Cell and Gene-Modified Cell Therapies

KYMRIAH (tisagenlecleucel)

YESCARTA

TECARTUS (brexucabtagene autoleucel) Suspension for IV infusion

Abecma

Breyanzi

RETHYMIC

StrataGraft

Gene Therapy

LUXTURNA voretigene neparvovec-rzyl for subretinal injection

zolgensma

ysis of Evaluate Pharma

[Cell and Gene Therapy: The Next Frontier in Healthcare]

Data until 2022

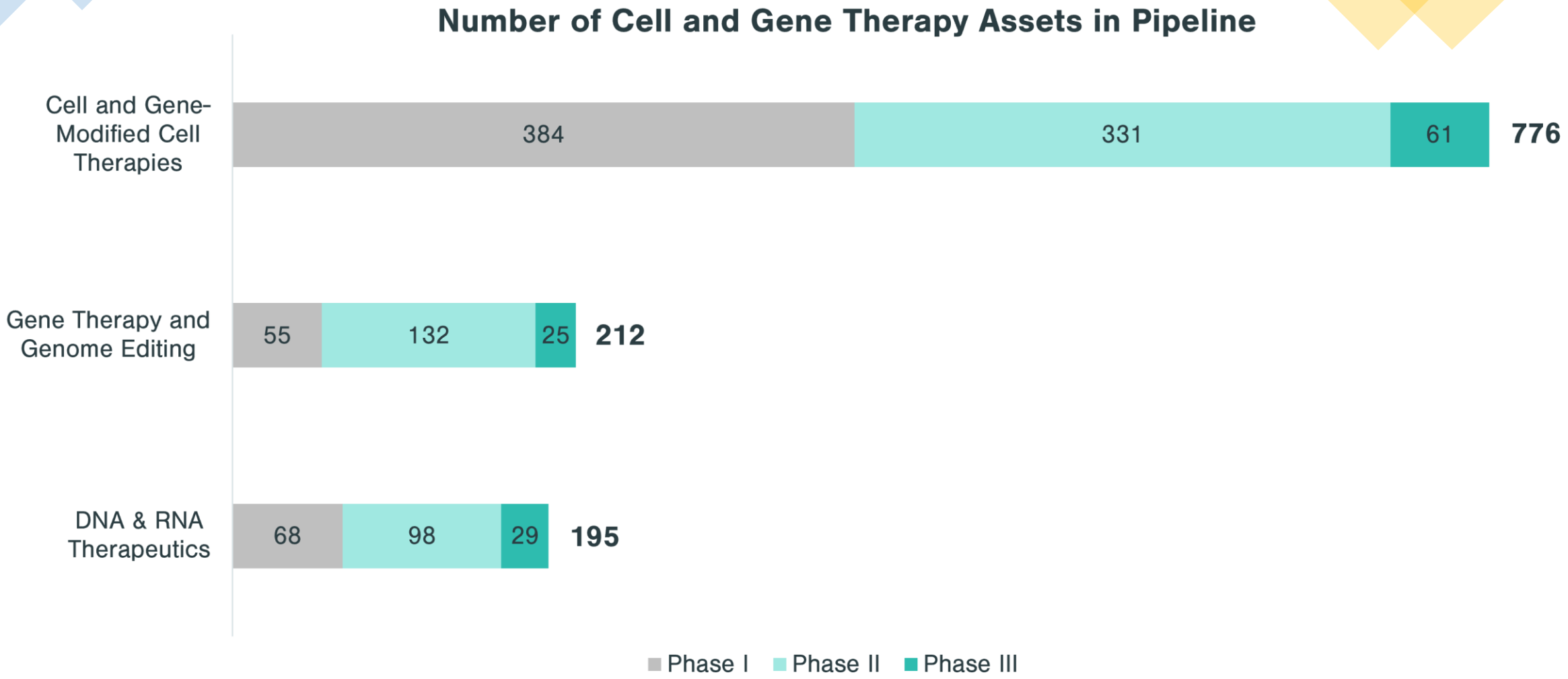

Source: Kx analysis of Evaluate Pharma

https://kxadvisors.com/wp-content/uploads/2022/06/CGT-Pipeline-Assets.png

Most Common Therapy Areas for CGT Assets in Pipeline

	Cell and Gene-Modified Cell Therapies	Gene Therapy and Genome Editing	DNA & RNA Therapeutics
Oncology	 62%	 12%	 28%
Central Nervous System	6%	 16%	 10%
Ophthalmology	2%	 17%	 7%
Gastro-Intestinal	2%	3%	 10%
Musculoskeletal	6%	 7%	5%
Total Assets	**776**	**212**	**195**

Source: Kx analysis of Evaluate Pharma

How can biomaterials enhance Cell&Gene therapy?

Biomaterials: Engineered materials (natural or synthetic) that enhance the delivery, stability, or function of therapeutic cells/genes.

Key roles include:

- Protecting nucleic acids from degradation (e.g., lipid nanoparticles for mRNA).
- Providing structural support for cell survival (e.g., hydrogels for stem cell delivery).
- Enabling targeted delivery (e.g., gold nanoparticles for tumor-specific CRISPR delivery)

Major types of nucleic acids for therapy

Major types of nucleic acids used to modulate cell behavior and could serve as therapeutic agents.

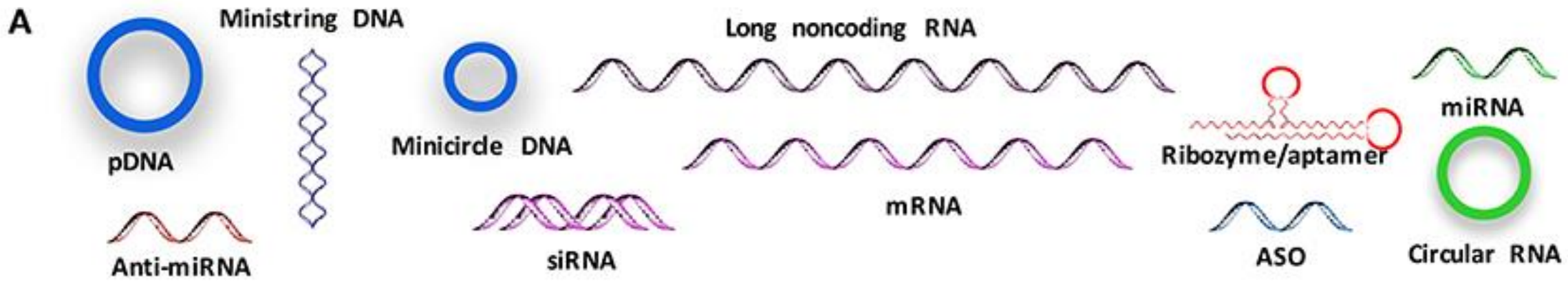

antisense oligonucleotides (ASO; 16–20 nucleotide long single-stranded DNAs)

https://doi.org/10.3389/fbioe.2019.00131

Intracellular trafficking and site of action for different types of nucleic acids

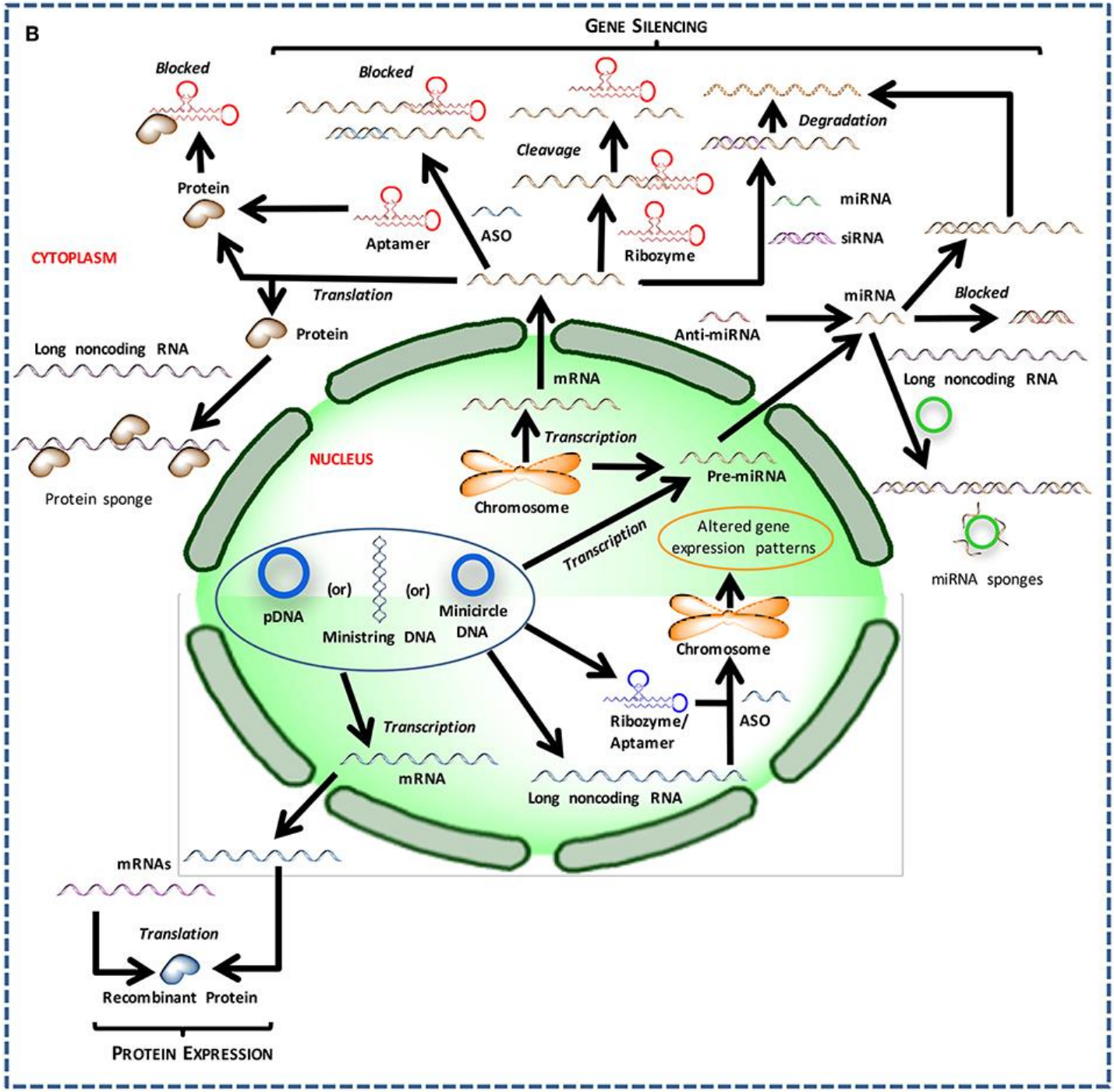

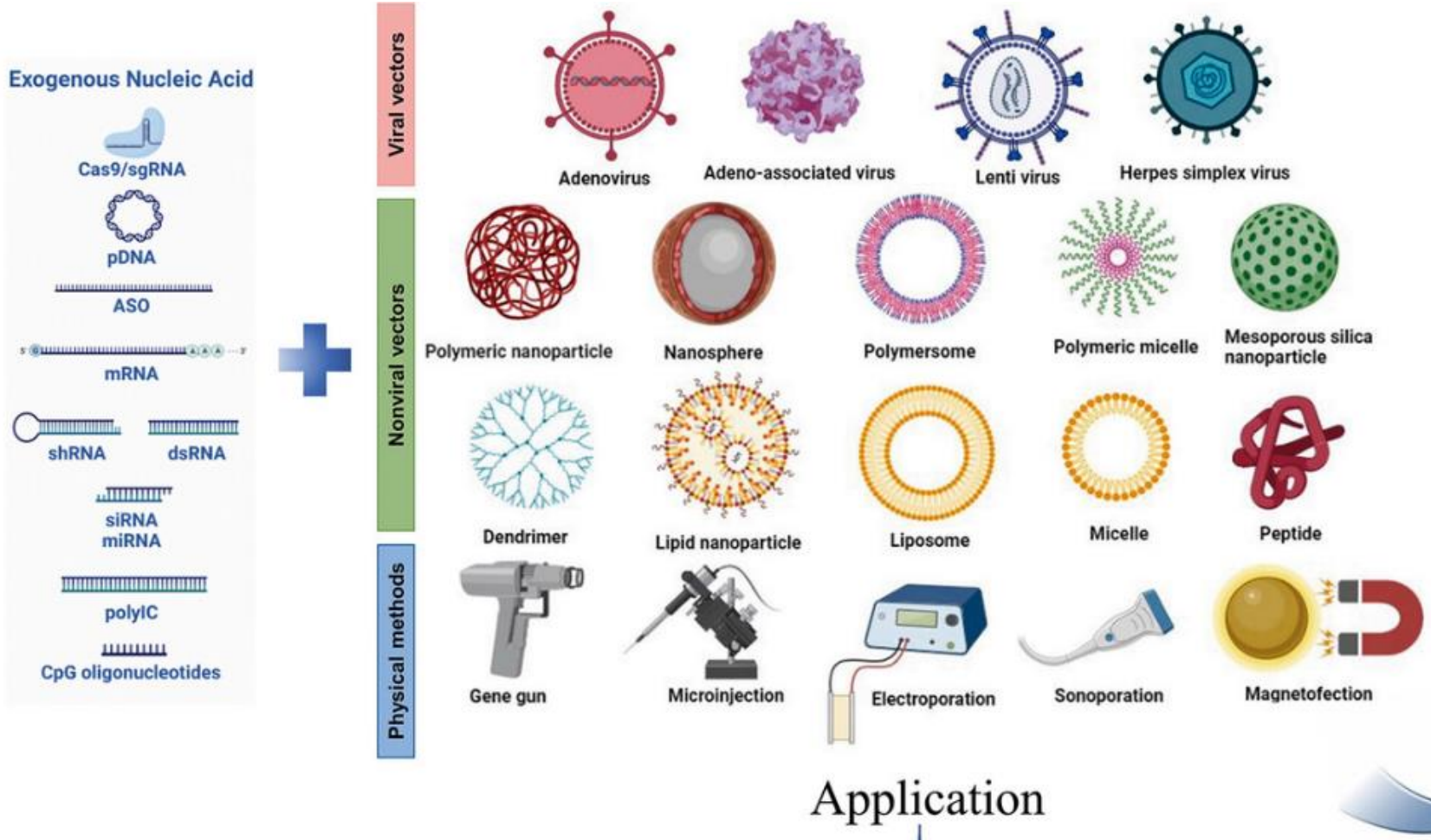

There are three methods available to address this obstacle:

(1) viral transduction;
(2) complexation with biological materials (non-viral vector)
(2) physical stimulation

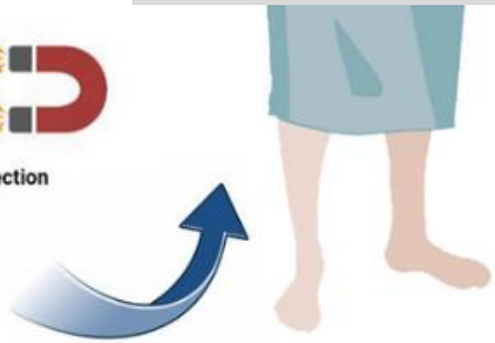

Application

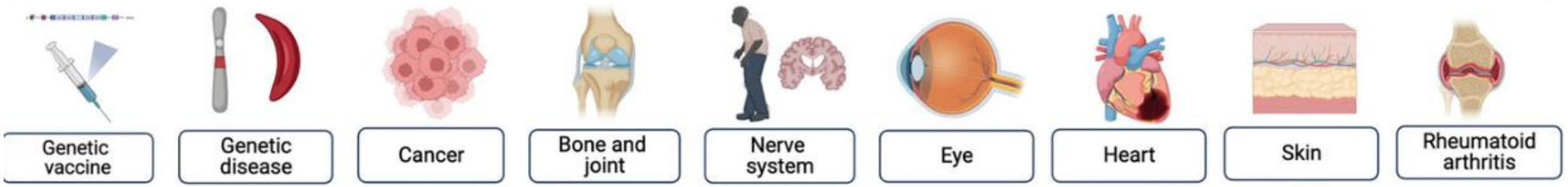

https://doi.org/10.1002/mco2.259

Physical methods

(A) PS laser setup and optical light pathway for **irradiation**.

(B) **Hydroporator**: hydrodynamic cell deformation-induced intracellular delivery of nanomaterials.

- (i) the design and operation principles
- (ii) The delivery mechanism
- (iii) layout of hydroporator
- (iv) High-speed microscope images
- (v) FITC-dextran in K562 cells using hydroporator.

(C) Principle of **magnetofection**

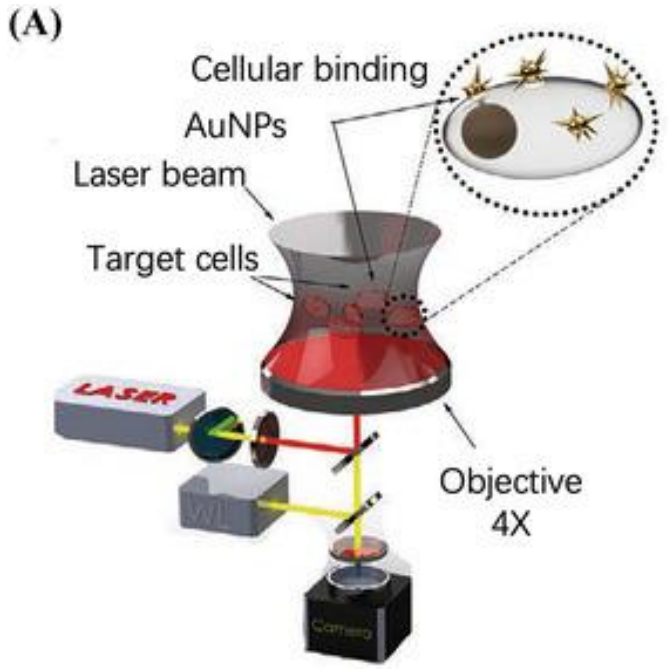

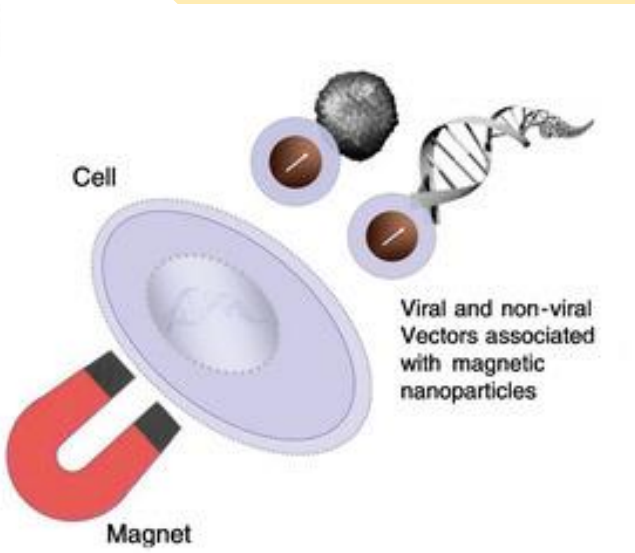

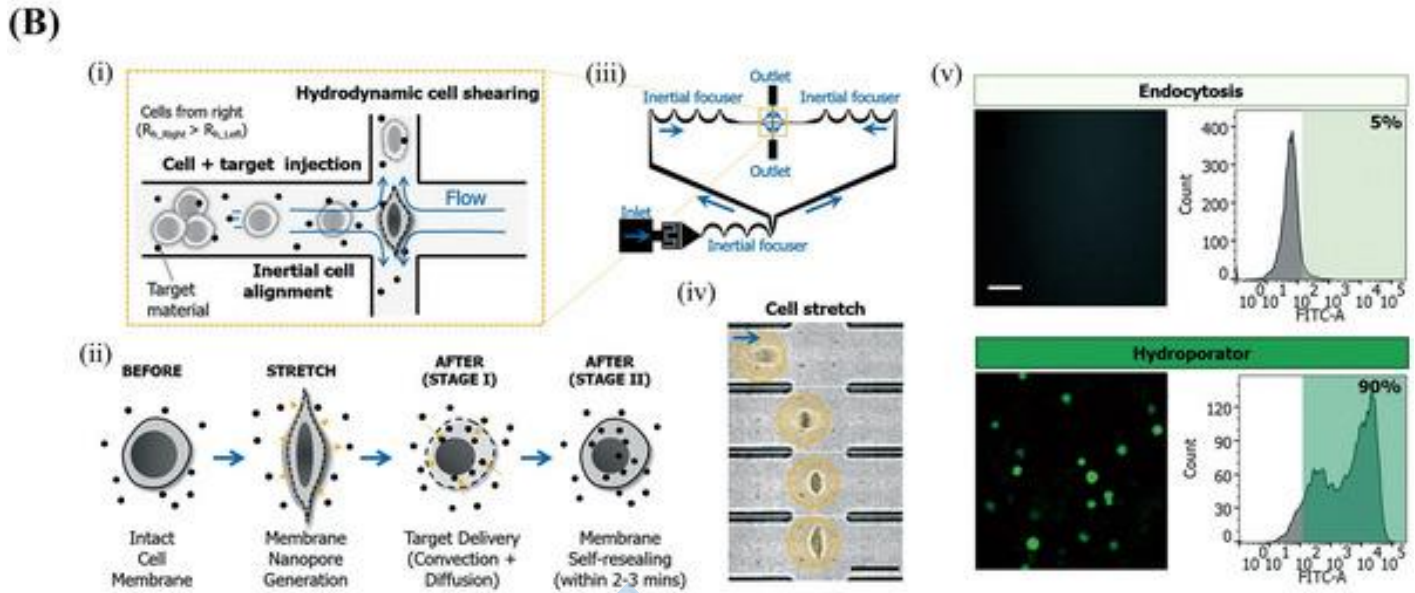

Viral vectors

Studies have shown that viral vector-mediated gene delivery is **the most efficient method of gene transfer**. Viral vectors are therefore the most commonly used gene therapy vectors. The production of nonpathogenic viruses for gene therapy has increased in recent years. These viruses include **retroviruses, lentiviruses, adenoviruses, and AAVs**.

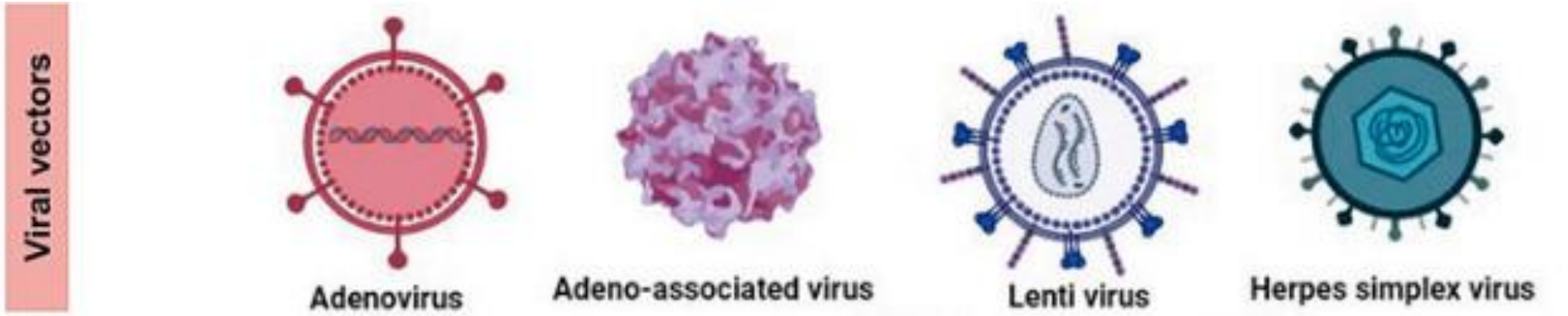

Nonviral vector delivery systems

three major categories: metallic, inorganic, and organic materials.

Including: liposomes and their derivatives, peptides, polymeric nanoparticles (polyesters, polyethyleneimine, PEG, polyamino acids, and natural polymers), inorganic nanoparticles, dendrimers, extracellular vesicles (EVs), and so on.

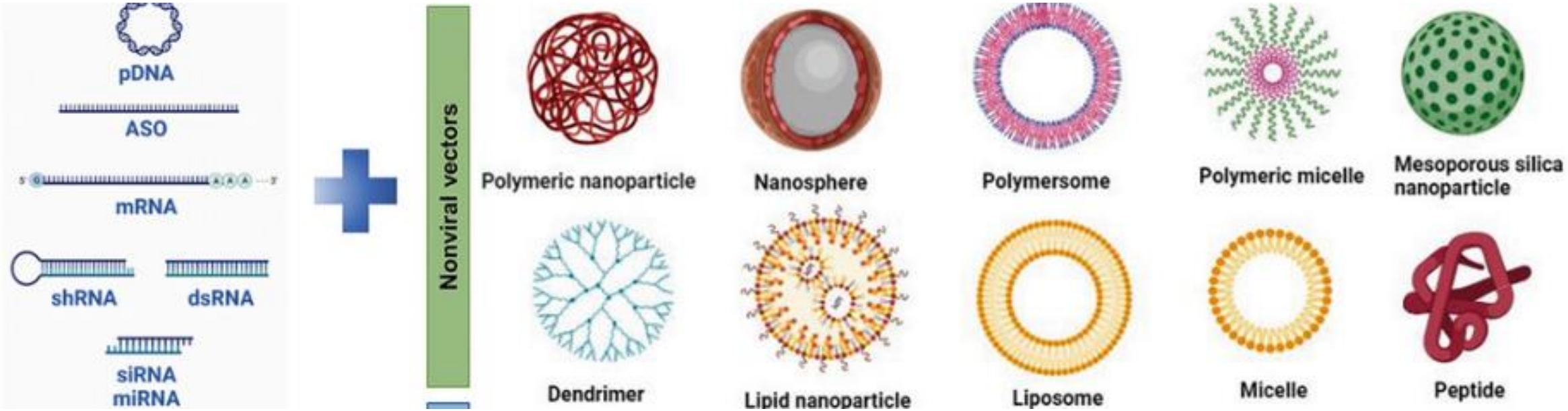

Examples

COVID-19 mRNA vaccines

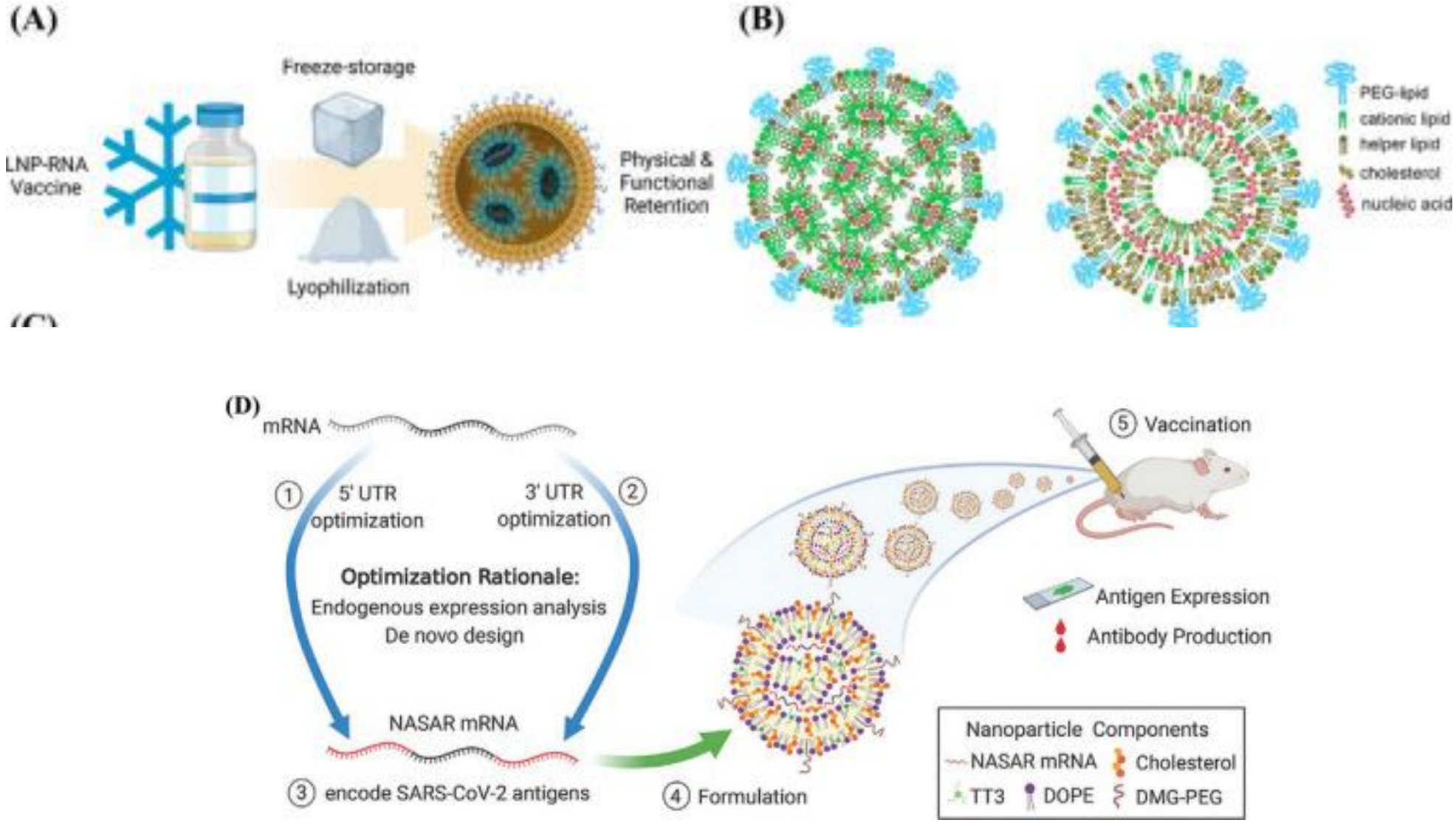

https://cdn.ncbi.nlm.nih.gov/pmc/blobs/78c3/10239531/8a014f3f1198/MCO2-4-e259-g002.jpg

Composition of Lipid nanoparticles (LNPs)

The Pfizer-BioNTech COVID-19 vaccine has not been approved or licensed by the U.S. Food and Drug Administration (FDA), but has been authorized for emergency use by FDA under an Emergency Use Authorization (EUA) to prevent Coronavirus Disease 2019 (COVID-19) for use in individuals 12 years of age and older.

https://www.pfizer.com/news/hot-topics/the_facts_about_pfizer_and_biontech_s_covid_19_vaccine

The ingredients are mRNA, lipids ((4-hydroxybutyl)azanediyl)bis(hexane-6,1-diyl)bis(2-hexyldecanoate), 2 [(polyethylene glycol)-2000]-N,N-ditetradecylacetamide, 1,2-Distearoyl-sn-glycero-3-phosphocholine, and cholesterol), potassium chloride, monobasic potassium phosphate, sodium chloride, dibasic sodium phosphate dihydrate, and sucrose.

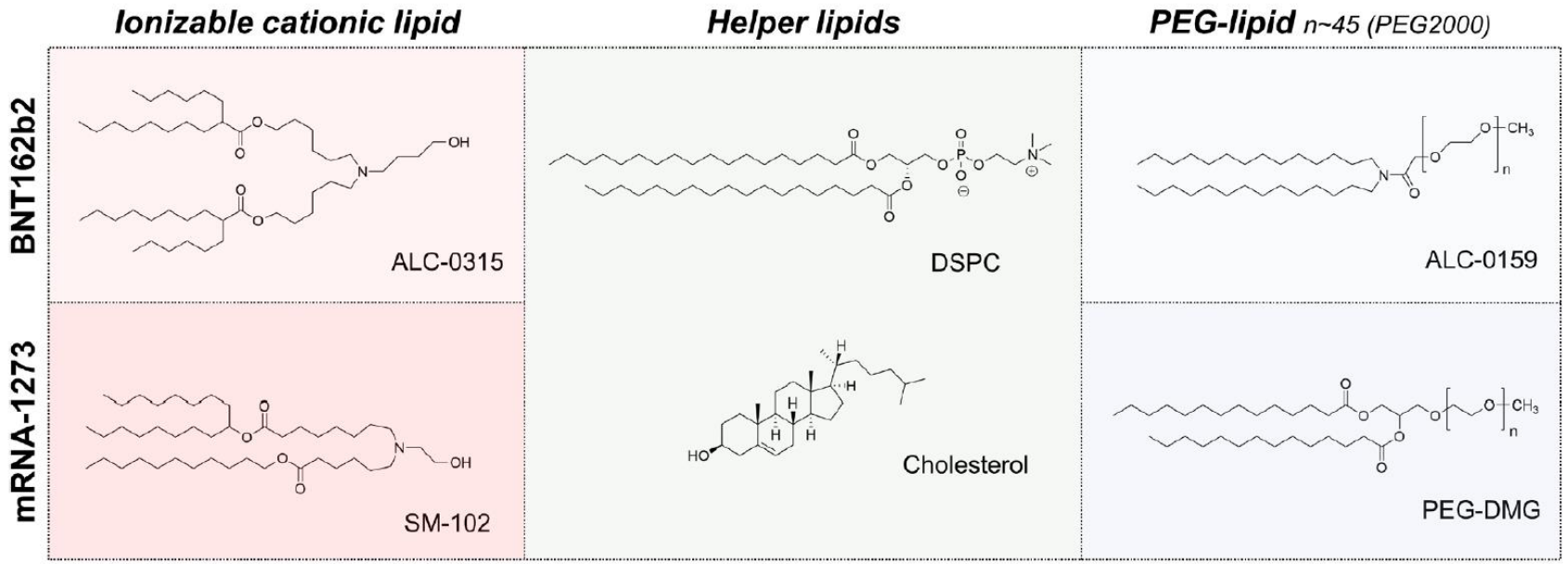

Fig. 6. Lipids used in the mRNA-LNP COVID-19 vaccines BNT162b2 (Comirnaty) and mRNA-1273.

Lipid nanoparticles (LNPs)

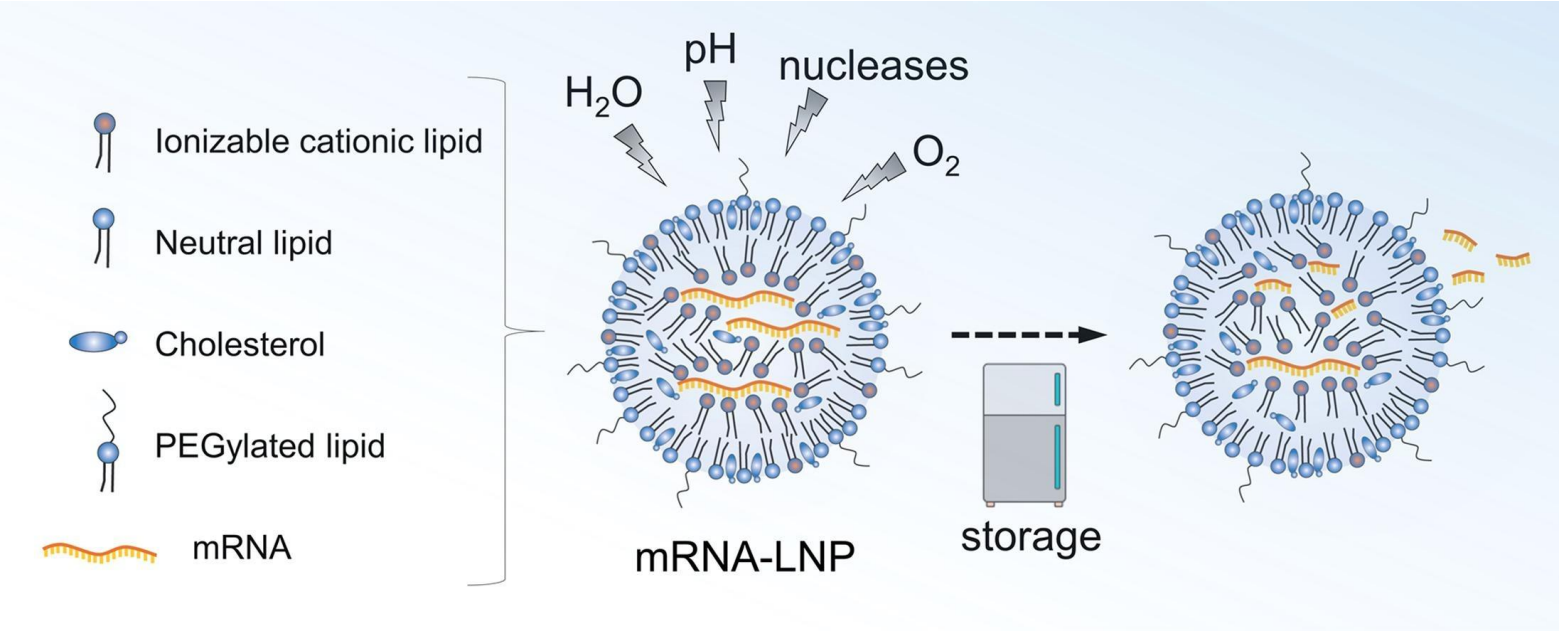

60–100 nm in size

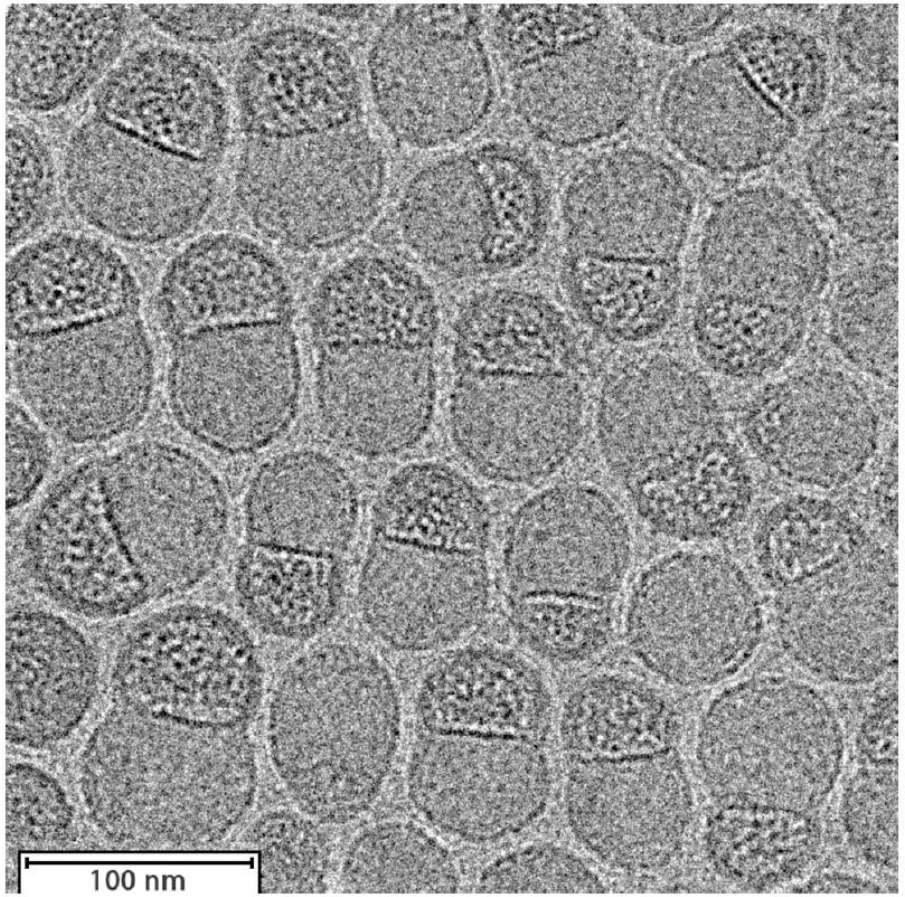

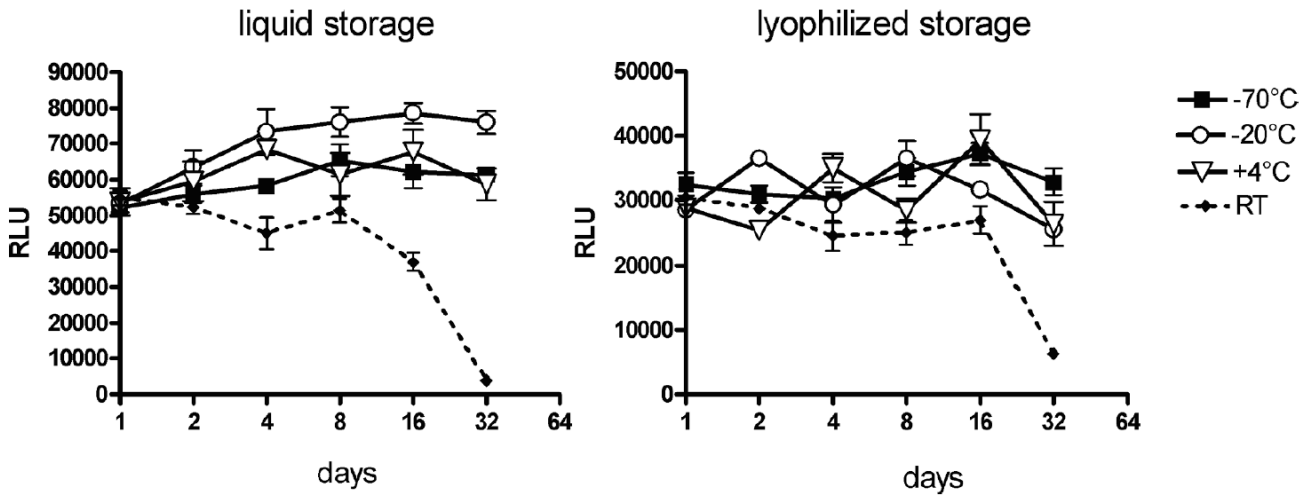

International Journal of Pharmaceutics 601 (2021) 120586

Peptide–poloxamine nanoparticles

Here, we show that peptides developed by modular design approaches can spontaneously form compact and monodisperse nanoparticles with poloxamines and nucleic acids via self-assembly. Both **messenger RNA and plasmid DNA** expression mediated by peptide-poloxamine nanoparticles are greatly boosted in vitro and in the lungs of cystic fibrosis mice with negligible toxicity.

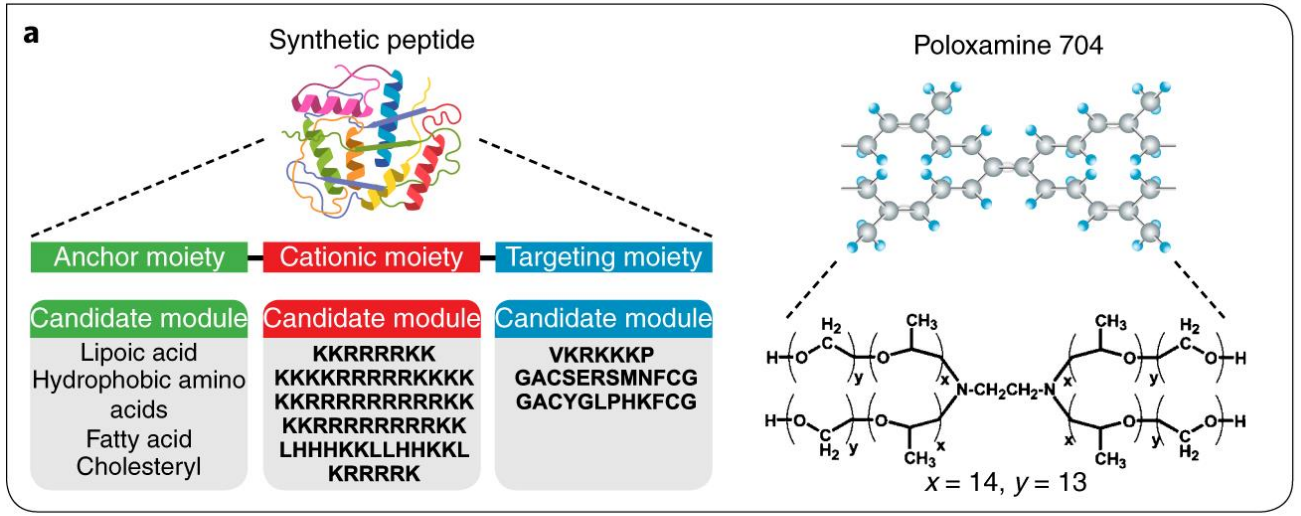

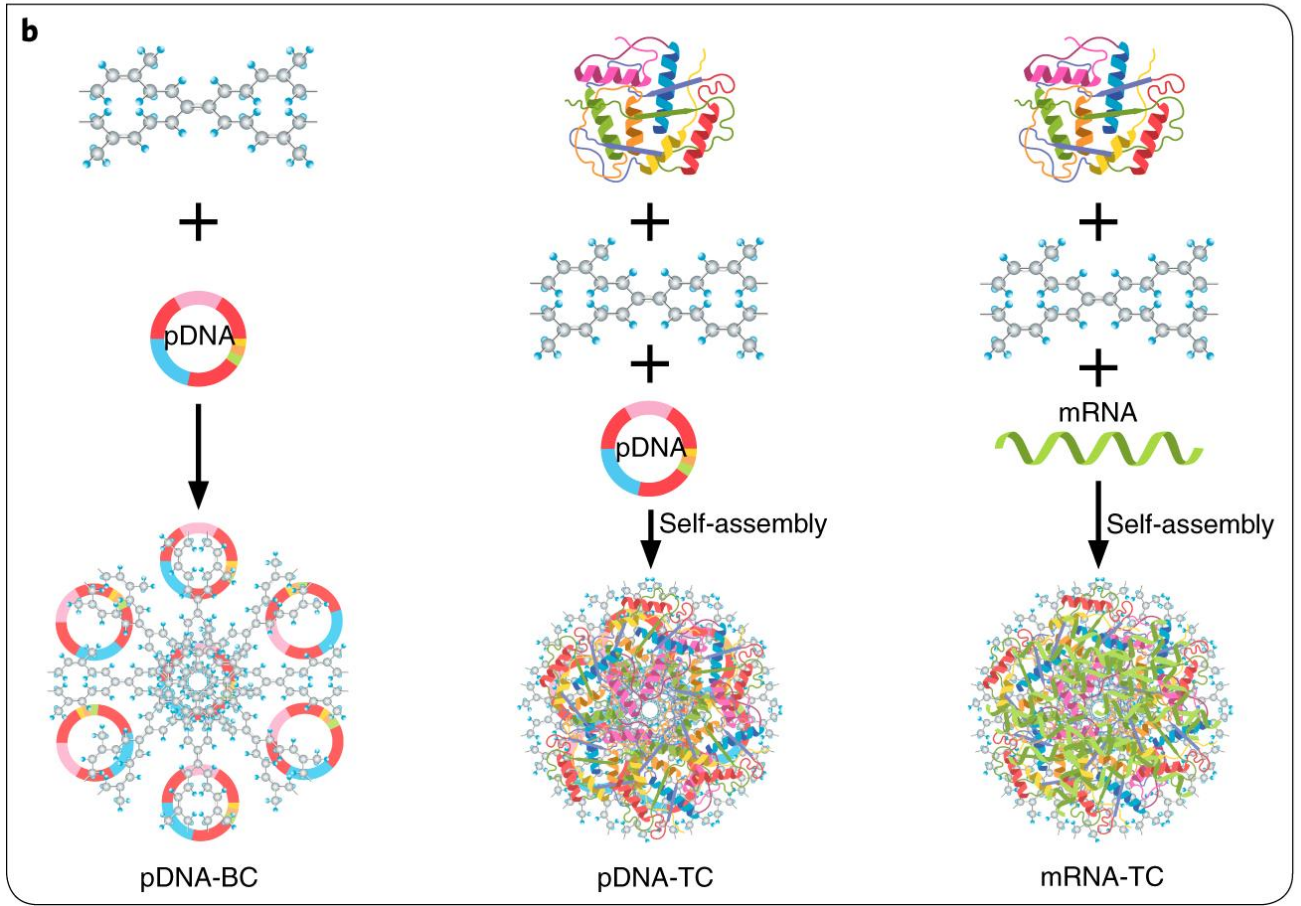

Nature Nanotechnology **volume 14**, pages287–297 (2019)

Peptide–poloxamine nanoparticles

Peptide–poloxamine nanoparticles containing integrating vectors enable successful in vitro and in vivo long-term restoration of cystic fibrosis transmembrane conductance regulator deficiency with a safe integration profile.

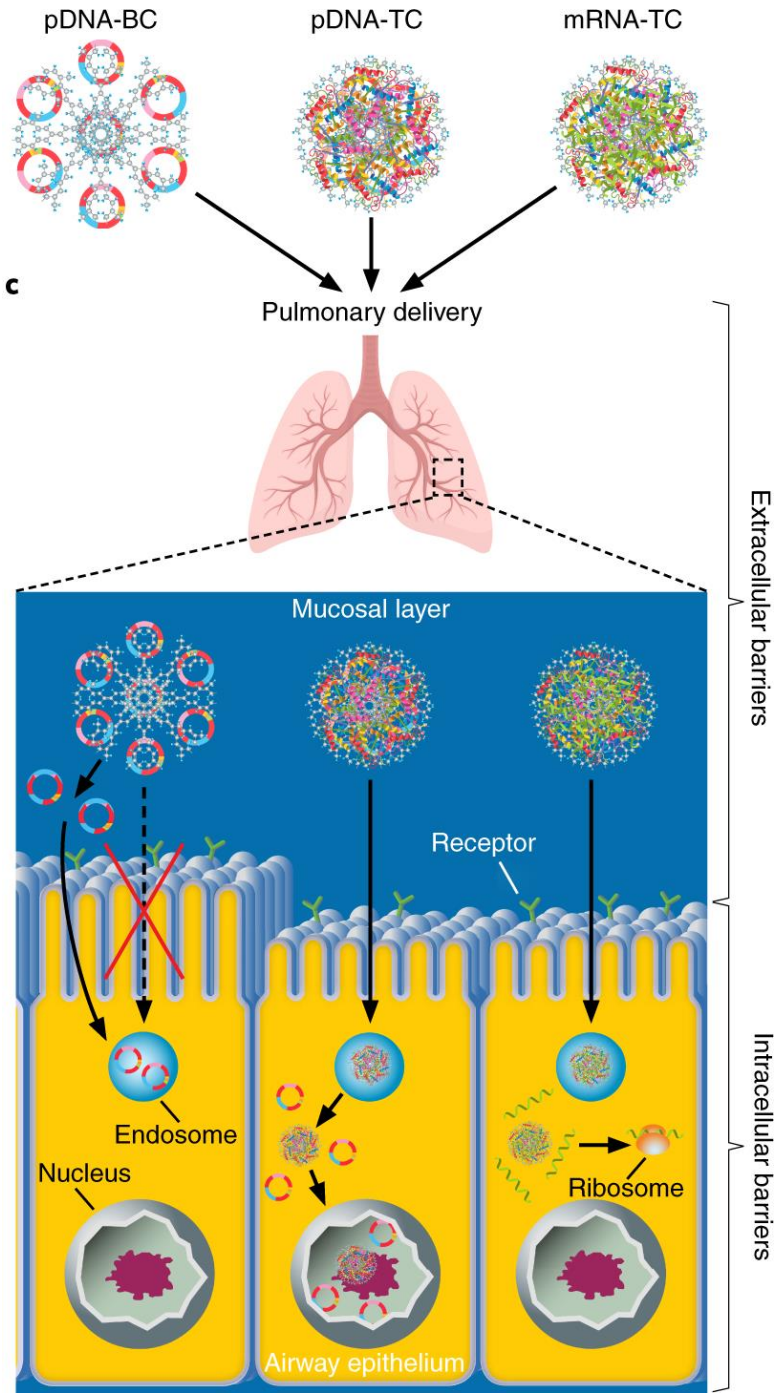

Nature Nanotechnology **volume 14**, pages287–297 (2019)

Peptide–poloxamine nanoparticles

Based on this hypothesis, we developed a platform of synthetic peptides consisting of **three functional moieties,** namely:

(1) **an anchor moiety** containing hydrophobic molecules used to interact with the hydrophobic blocks of T704;
(2) **a cationic moiety** comprising several basic amino acids to condense nucleic acids and facilitate efficient endosomal escape;
(3) **a targeting moiety** that actively directs the nucleic acid payloads to target cells or specific organelles.

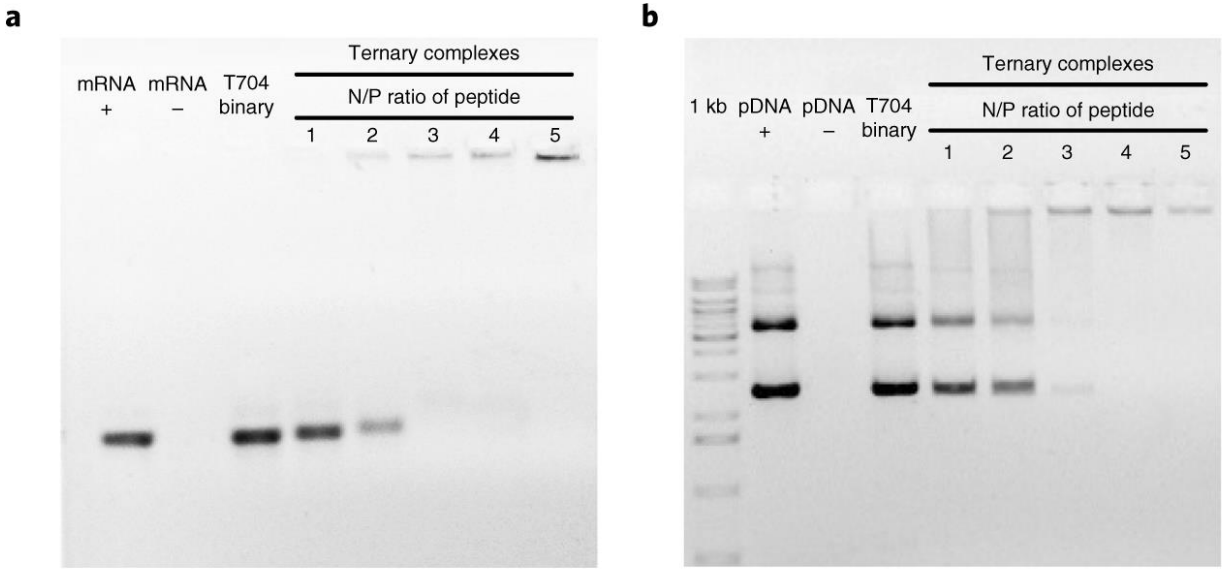

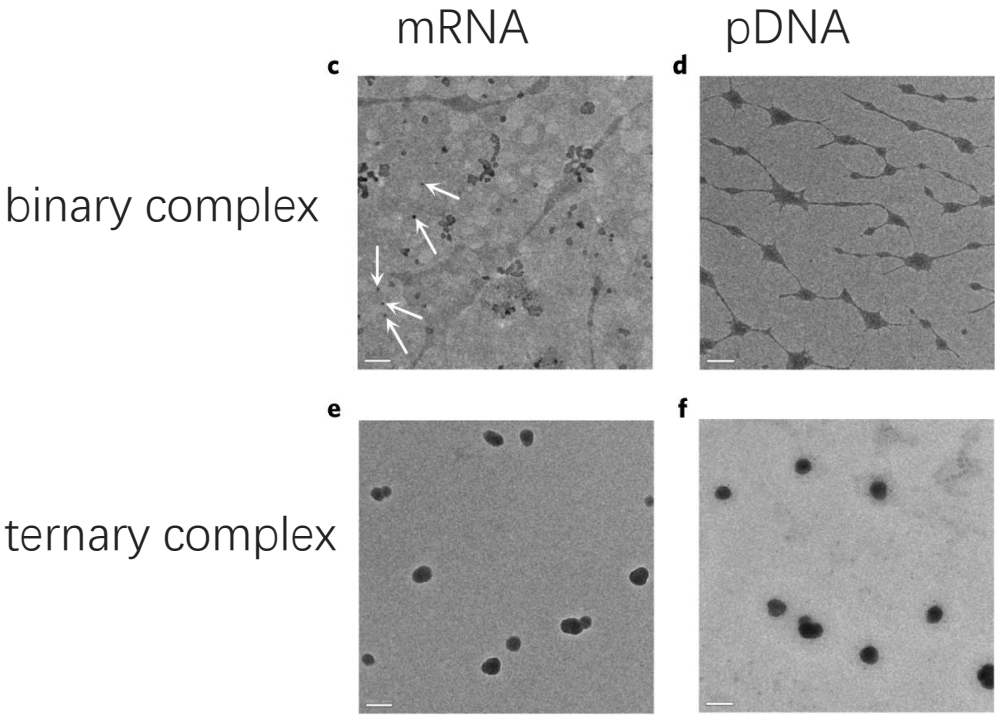

Nature Nanotechnology **volume 14**, pages287–297 (2019)

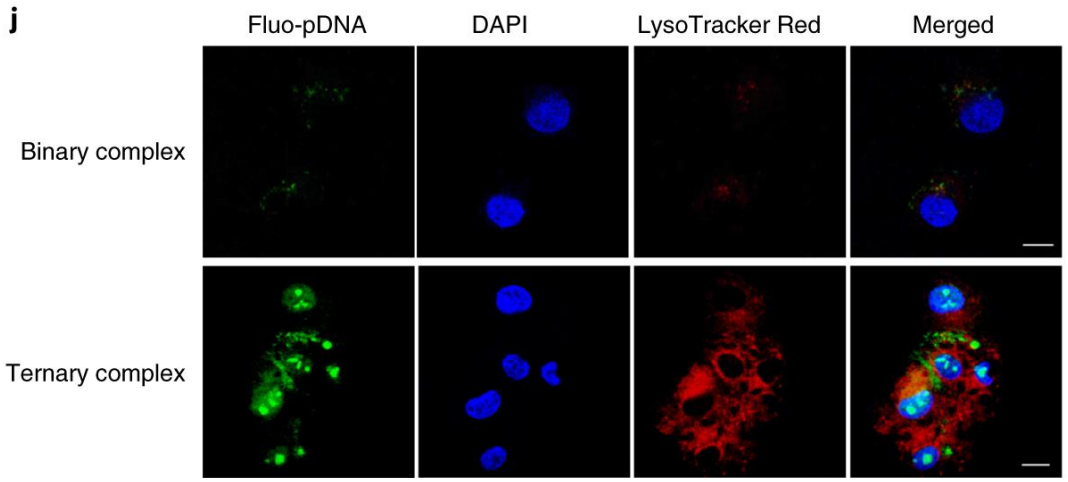

j, Subcellular location of the Fluo-pDNA/T704 binary complex and Fluo-pDNA/T704/peptide 0 ternary complex after 4 h incubation with 16HBE cells obtained by confocal laser scanning microscopy.

Green channel, Fluo-pDNA; blue channel, nuclei stained by DAPI; red channel, endocytic vesicles marked by LysoTracker Red DND-99; merged, combination of the aforementioned channels. Scale bars: 10 μm.

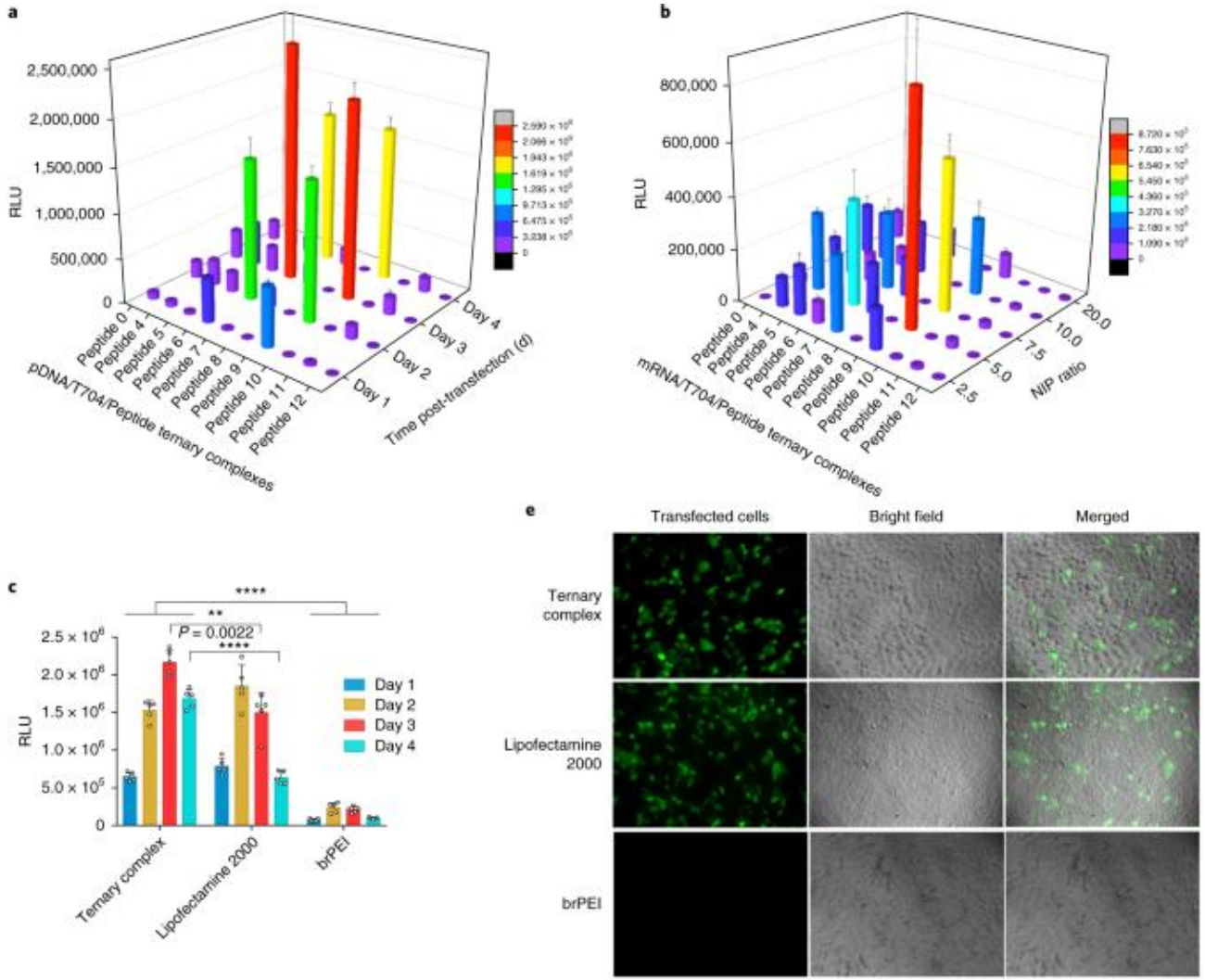

a,**b**, Transfection efficiency of pDNA-based (in the optimum composition) (**a**) or mRNA-based ternary complexes comprising different peptides in 16HBE cells (**b**). The luciferase activity was expressed as relative light units (RLU). **c**,**d**, Comparisons of the in vitro transfection efficiency mediated by optimized pDNA/T704/peptide 9 (**c**) and mRNA/T704/peptide 9 ternary complexes (**d**) and other non-viral counterparts in 16HBE cells. **e**, Representative expression of EGFP-mRNA mediated by the ternary complex, Lipofectamine 2000 lipoplex and brPEI polyplex in 16HBE cells.

Nature Nanotechnology **volume 14**, pages287–297 (2019)

Application to treat Cystic fibrosis

Cystic fibrosis, which is caused by mutations in the gene encoding the **cystic fibrosis transmembrane conductance regulator (CFTR)**[1], has been the subject at the forefront of these diseases.

cystic fibrosis bronchial epithelial cells (CFBE-delF)

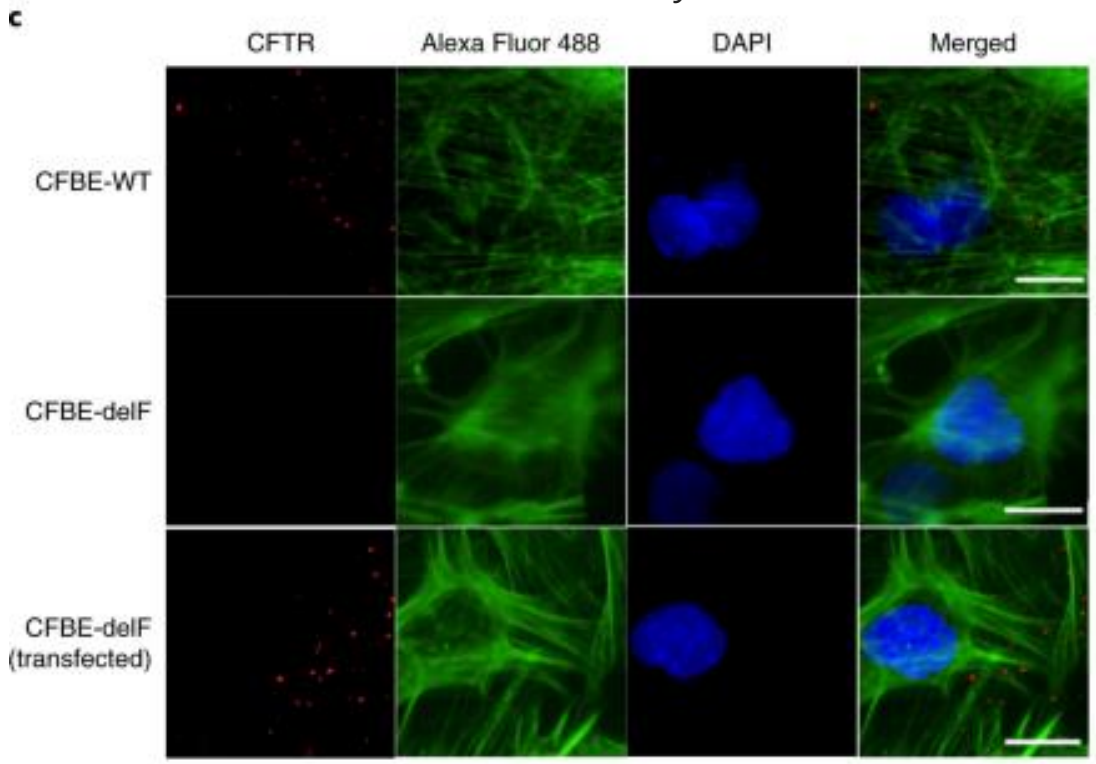

c, Confocal laser scanning microscopy images of untreated CFBE-WT cells (first row), untreated CFBE-delF cells (second row) and pGM206-fLUC-CFTR/T2 + *SB*100X-mRNA-transfected CFBE-delF cells (third row, two weeks after transfection) with CFTR-antibody staining. For each panel, the images from left to right show CFTR proteins (red), F-actin (Alexa Fluor 488 phalloidin, green), nuclei (DAPI, blue) and an overlay of the three images. Scale bars: 20 μm.

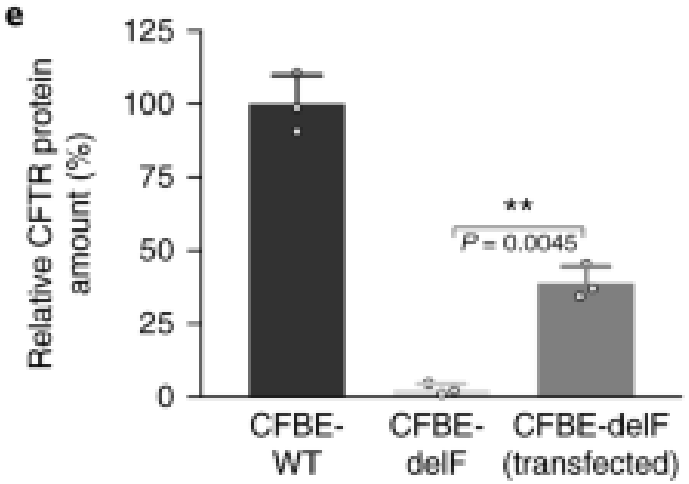

e, Semi-quantitative evaluation of the relative amount of CFTR protein in western blot analysis ($n = 3$ independent experiments). The amount of the CFBE-WT control protein was normalized to 100%.

Nature Nanotechnology **volume 14**, pages287–297 (2019)

a, Stable and long-term luciferase reporter gene expression in mouse lungs mediated by the *SB* transposon system (pGM206-fLUC-CFTR/T2 + *SB*100X-mRNA).
b, Bioluminescence intensity.
c, Luciferase activity in lung homogenates of mice 2 or 18 weeks after dosing.

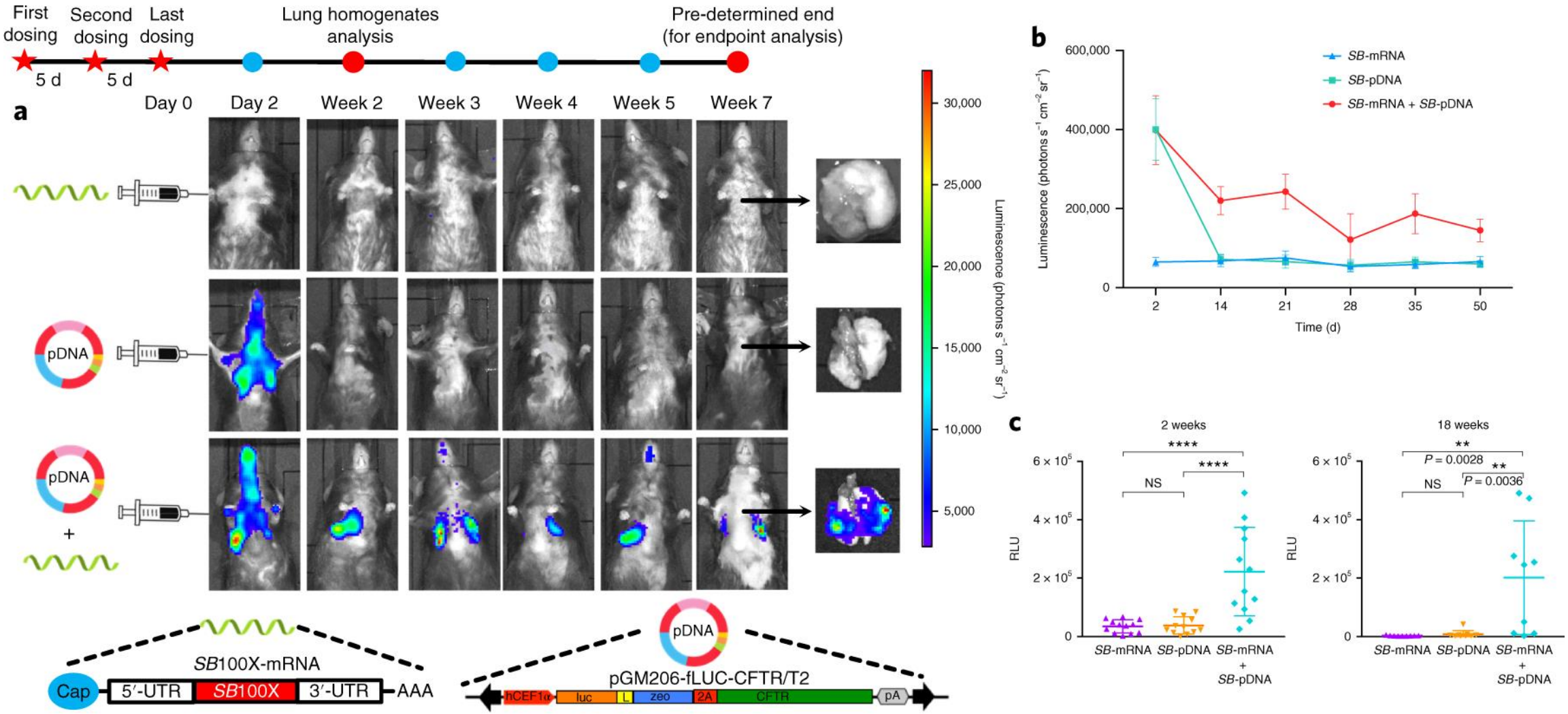

Nature Nanotechnology **volume 14**, pages287–297 (2019)

CRISPR-Cas9 genome editing

The system consists of two essential parts:

-the Cas9 enzyme, which functions as molecular scissors

-the CRISPR array, which is made up of short, repetitive DNA sequences interspersed with distinctive “spacer” sequences generated from previous viral contacts

the transcription of the CRISPR array into precursor molecules, which are subsequently transformed into distinct **guide RNAs (gRNAs)**. Every gRNA is designed to work in conjunction with a particular target DNA sequence.

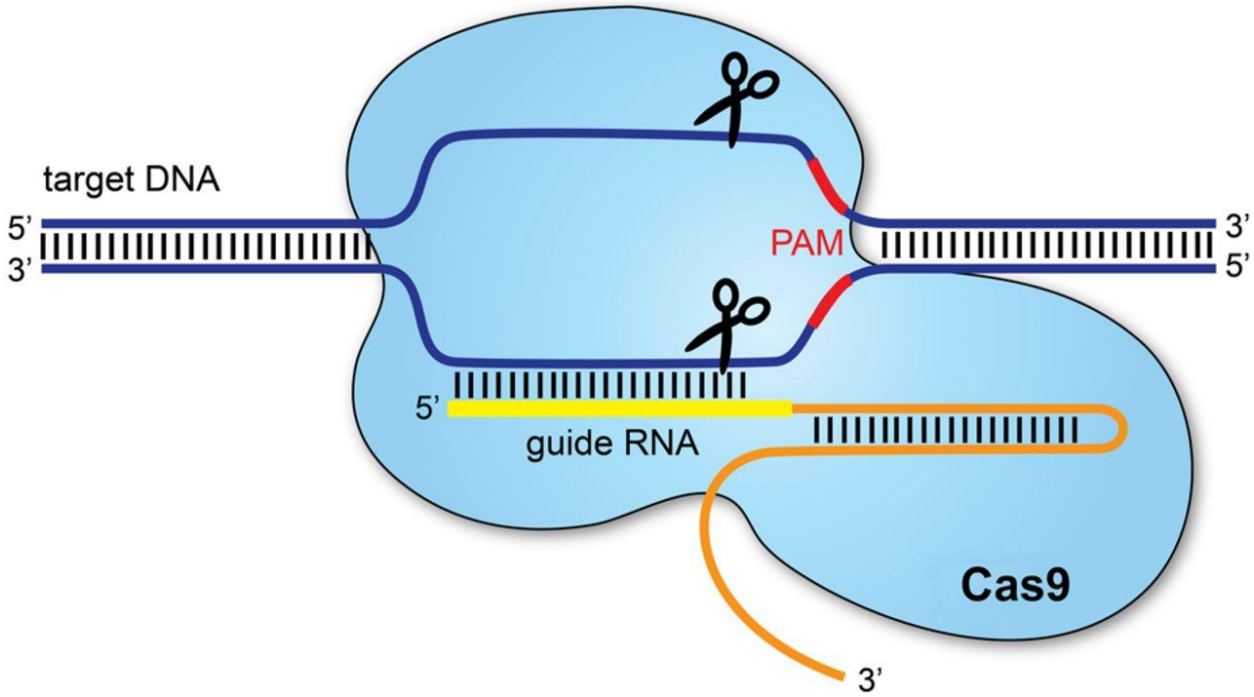

Year	Discovery/Event	Description	Reference
1987	Discovery of CRISPR	Japanese researchers describe "clustered regularly interspaced short palindromic repeats" (CRISPR) in *E. coli*	Ishino et al. (1987)
2005	First Evidence of CRISPR Function	Scientists demonstrate that CRISPR sequences play a role in bacterial immunity against phage infections	Barrangou et al. (2007)
2007	Identification of tracrRNA	Researchers discovered trans-activating CRISPR RNA (tracrRNA), which is part of the bacterial immune system	Deltcheva et al. (2011)
2011	CRISPR/Cas9 Genome Editing	Jennifer Doudna and Emmanuelle Charpentier propose using CRISPR/Cas9 for RNA-guided genome editing in bacteria	Jinek et al. (2012)
2012	CRISPR/Cas9 Editing in Eukaryotic Cells	George Church's lab demonstrates efficient CRISPR/Cas9 genome editing in mammalian cells	Cong et al. (2013); Mali et al. (2013)
2013	Dual RNA Guided Cas9 System	Zhang Feng's lab published a paper describing the use of the CRISPR/Cas9 system for precise genome editing in eukaryotic cells	Ran et al. (2013)
2014	RNA Editing with Catalytically Dead Cas9	Researchers developed a version of Cas9 with inactivated nuclease activity, known as "dead" Cas9 (dCas9), for RNA targeting and regulation	Hsu et al. (2014)
2015	Base Editing with CRISPR/Cas9	David Liu's lab introduces base editing, allowing specific nucleotide changes without causing double-strand breaks	Komor et al. (2018)
2016	CRISPR/Cas9 *In Vivo* Gene Editing	Scientists use CRISPR/Cas9 for successful gene editing directly within living animals	Cyranoski (2016)
2017	Clinical Trials for Genetic Disorders	The first clinical trials using CRISPR/Cas9 are initiated to treat genetic disorders like beta-thalassemia and sickle cell anemia	Frangoul et al. (2021); NCT03655678; NCT03745287
2018	Prime Editing	David Liu and Doudna's labs develop prime editing, a versatile genome editing technique allowing precise insertion, deletion, and substitution	Lapinaite et al. (2020)
2019	*In Vivo*, CRISPR/Cas9 Editing in Humans	Researchers in China report the use of CRISPR/Cas9 to edit genes within the human body for the first time in clinical trials	Lu et al. (2020)
2020	Nobel Prize in Chemistry Awarded	Jennifer Doudna and Emmanuelle Charpentier received the Nobel Prize in Chemistry for the development of CRISPR/Cas9 genome editing	Westermann et al. (2021)
2021	Continued Clinical Trials and Therapeutic Applications	Clinical trials and research continue, exploring CRISPR/Cas9's potential in treating various genetic and acquired diseases	Li et al. (2020); Liu et al. (2021a); NCT03872479

https://doi.org/10.3389/fchem.2023.1259435

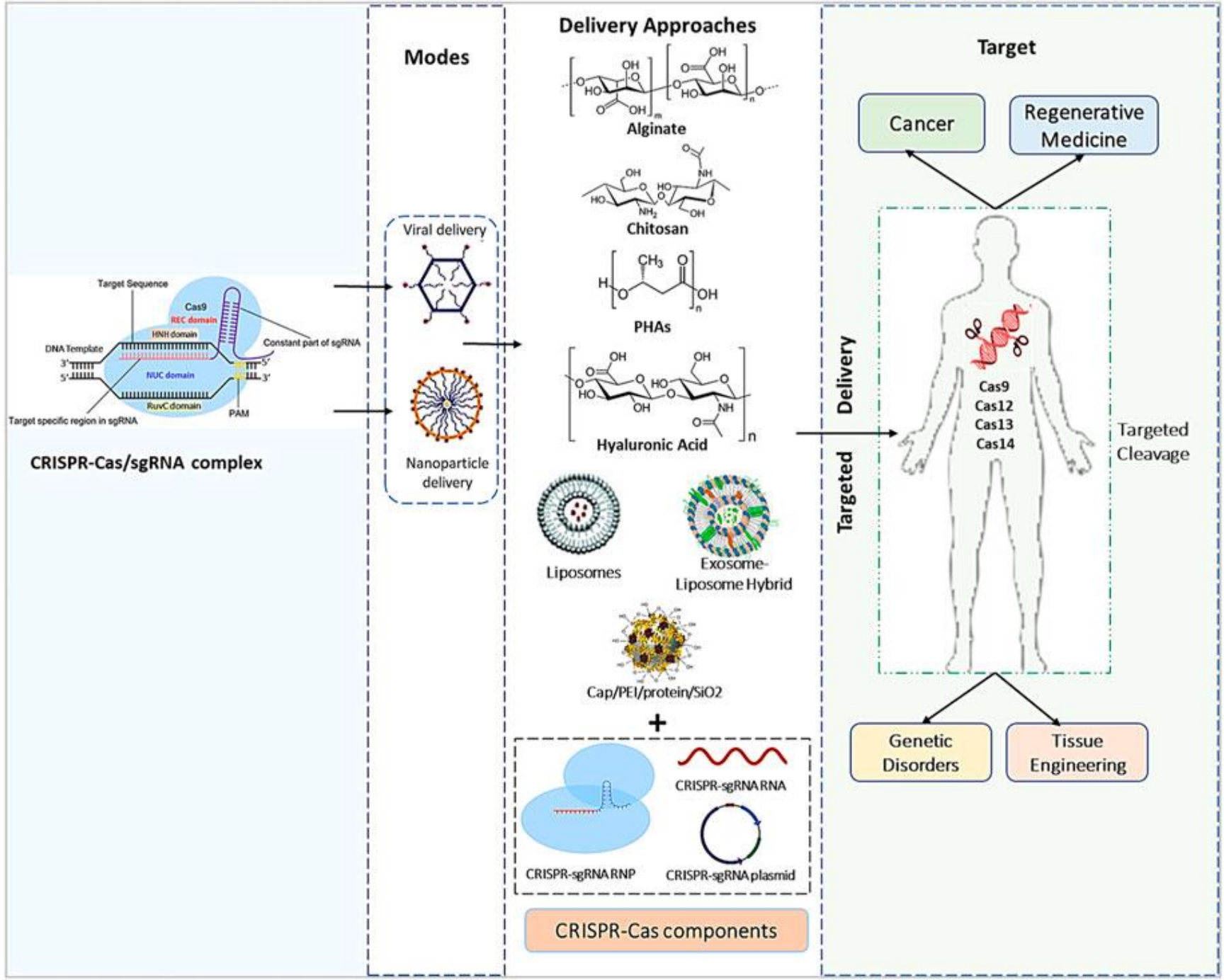

https://www.frontiersin.org/files/Articles/1259435/fchem-11-1259435-HTML-r1/image_m/fchem-11-1259435-g002.jpg

Exosomes for delivery of Cas9 ribonucleoprotein (RNP)

Delivery of **Cas9 ribonucleoprotein (RNP)** owns competitive advantages over other options; however, the large size of RNPs exceeds the loading capacity of currently available delivery vectors.

In this study, we developed a method where Cas9 RNP can be loaded into **exosomes from hepatic stellate cells (HSCs; LX-2)** for the treatment of different liver disorders.

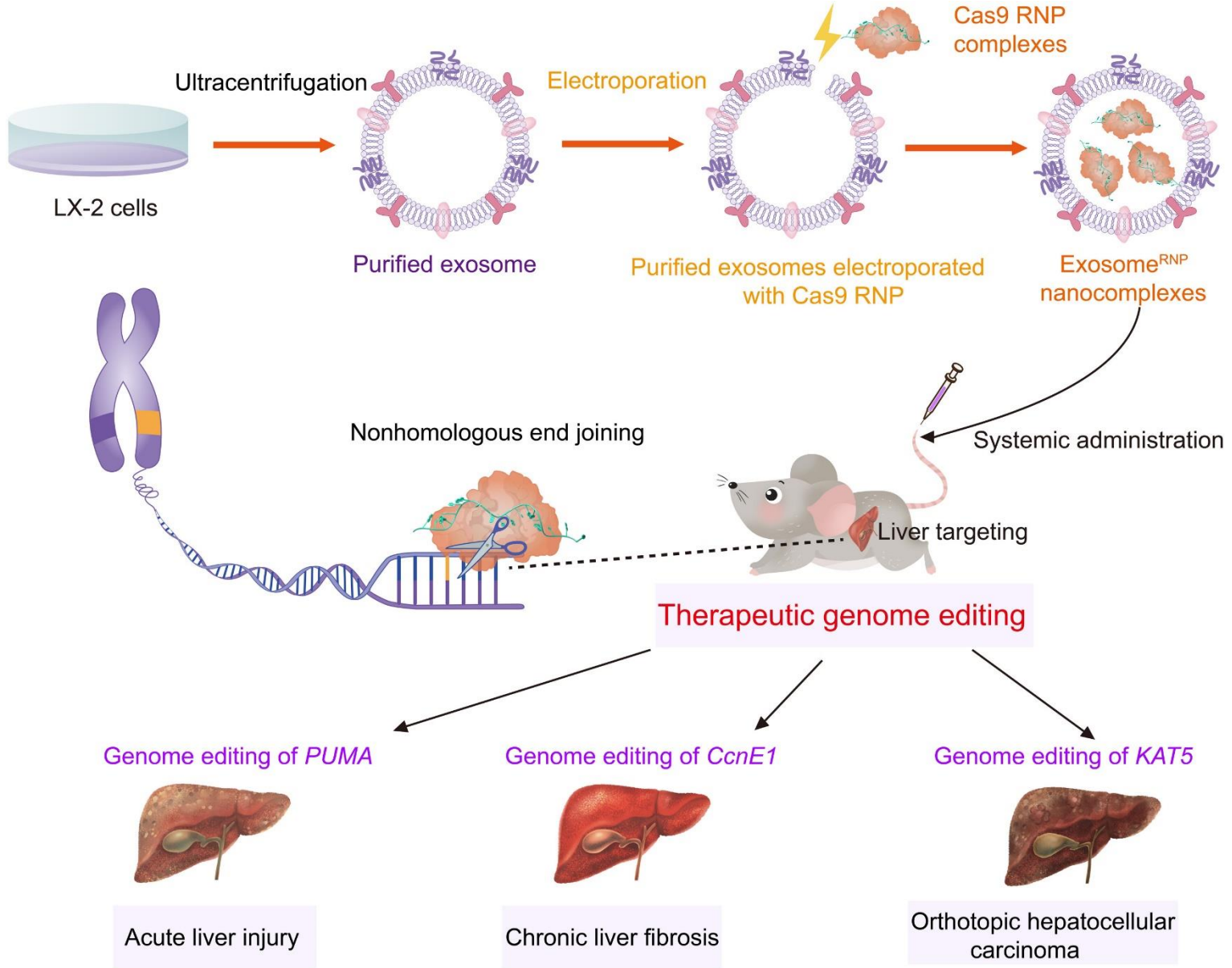

*Sci. Adv.***8**,eabp9435(2022).DOI:10.1126/sciadv.abp9435

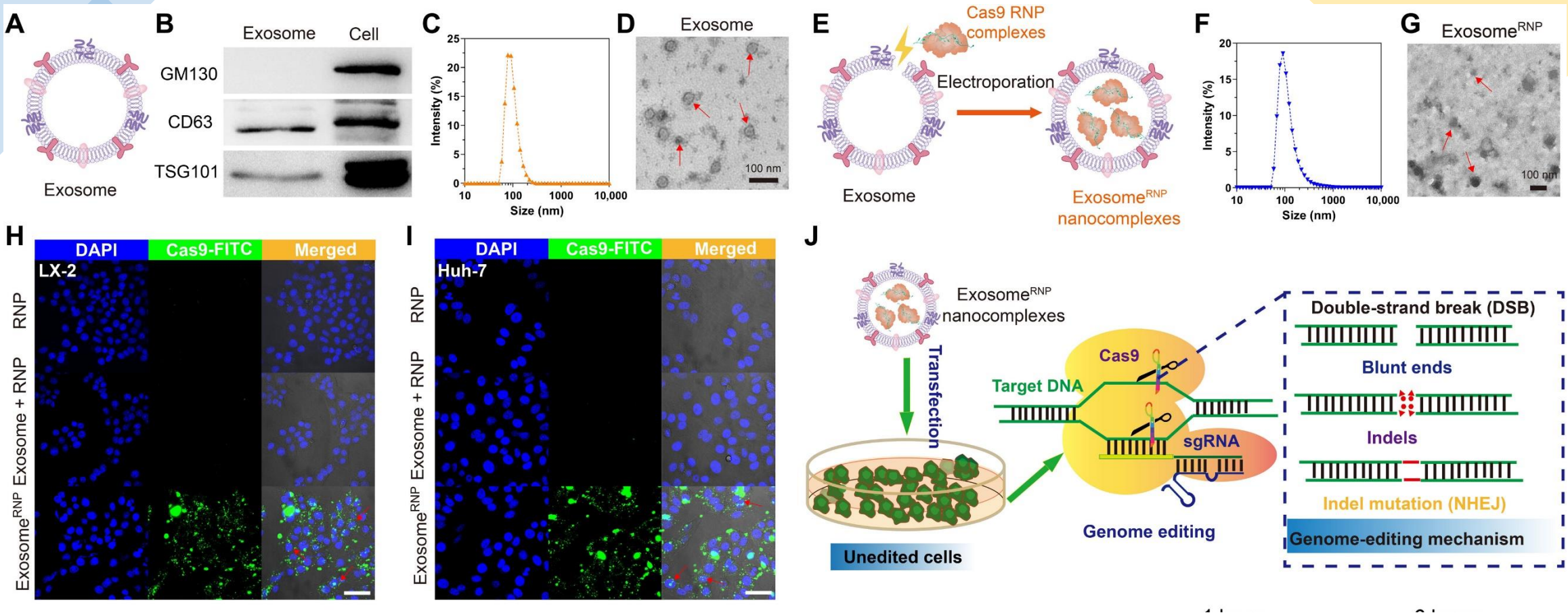

Characterization of purified exosome (**A**) and exosome^{RNP} complexes (**E**). (**B**) Biomarkers of exosome by western blotting. (**C** and **D**) DLS and TEM the image of purified exosome. The arrows show the typical exosome nanoparticles. (**F** and **G**) DLS and TEM image of exosome^{RNP} complexes. The arrows show the typical exosome^{RNP} nanoparticles. (**H** and **I**) Cytosolic delivery of Cas9-FITC into LX-2 (H) and Huh-7 (I) cells by exosomes for 4 hours.
(**J**) Exosome-mediated Cas9 RNP delivery for genome editing.

*Sci. Adv.***8**,eabp9435(2022).DOI:10.1126/sciadv.abp9435

Application to treat acute liver failure

A single overdose of **acetaminophen (APAP)** or therapeutic misadventure is the leading cause of drug-induced **acute liver failure** (*46*, *47*). Recently, Zhang and co-authors (*48*) have found that **p53 up-regulated modulator of apoptosis (*PUMA*)** plays a critical role in APAP-induced liver injury and is markedly induced after APAP treatment. Thus, for the therapy of acute liver injury, we designed **sgRNA-targeting *PUMA* and delivered exosome^{RNP}** to investigate its therapeutic efficacy for the acute liver injury (Fig. 3A).

(Acetaminophen is a pain reliever and a fever reducer.)

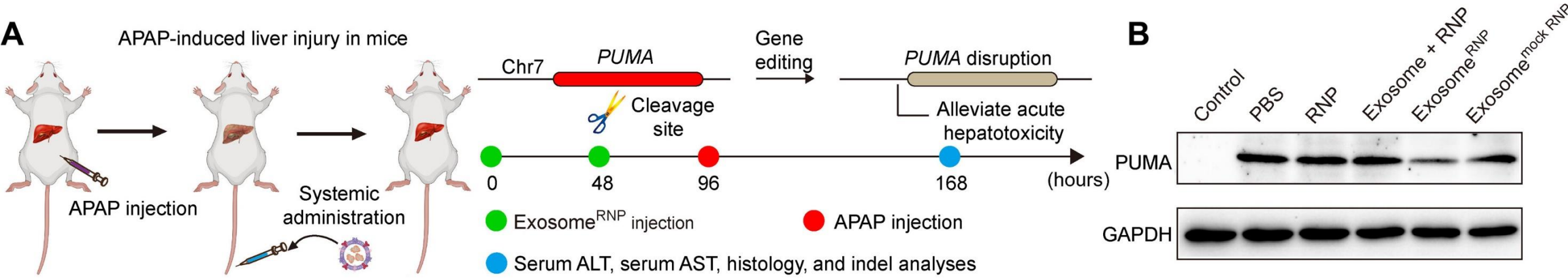

*Sci. Adv.***8**,eabp9435(2022).DOI:10.1126/sciadv.abp9435

(**E** and **F**) Serum AST (E) and ALT (F) levels in mice after the specified treatments.

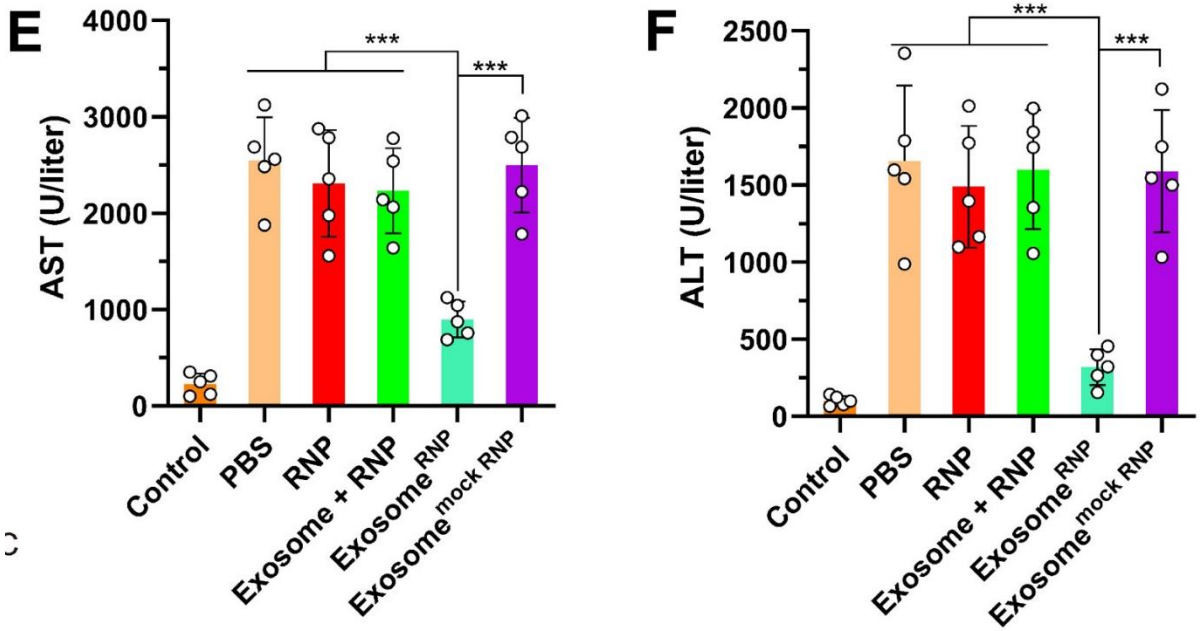

(**M**) Survival rates of mice after the specified treatments.

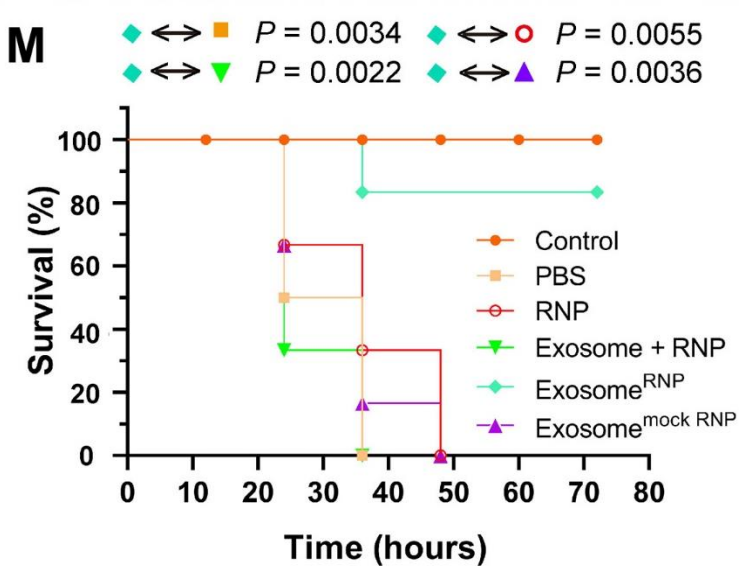

*Sci. Adv.***8**,eabp9435(2022).DOI:10.1126/sciadv.abp9435

Application to treat hepatocellular carcinoma (HCC)

Because of the high recurrence rate and lack of effective therapy options, HCC is often associated with poor patient survival (*54*–*56*). New therapeutic options for HCC, including CRISPR-based technologies (*57*), have attracted wide attention in recent years. **K (lysine) acetyltransferase 5 (*KAT5*)** is required for HCC growth, and disruption of *KAT5* inhibited tumor growth both in vitro and in vivo (*58*). Therefore, we designed **sgRNA-targeting *KAT5* and developed exosome^{RNP}** to treat HCC (Fig. 6A).

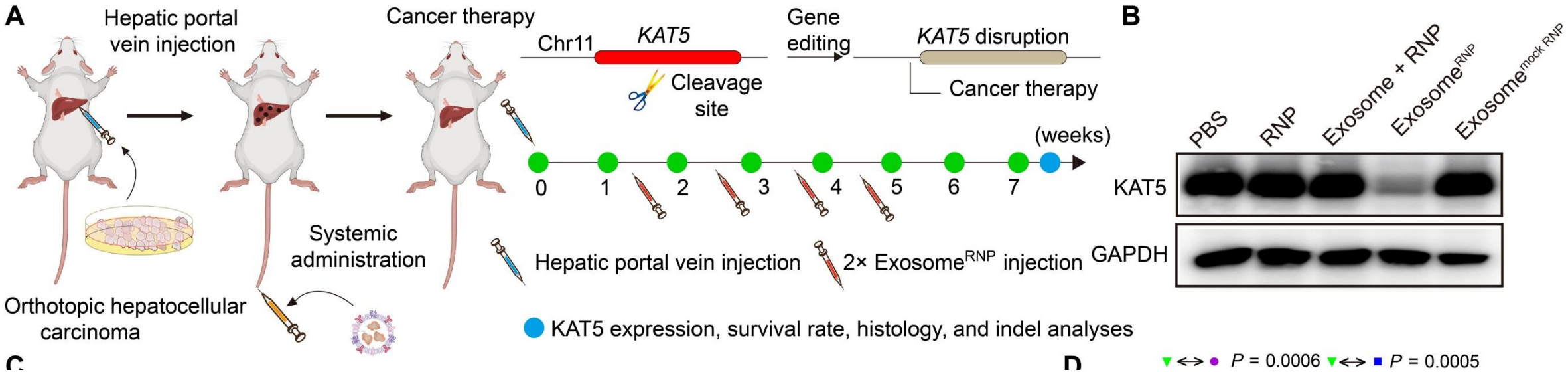

*Sci. Adv.***8**,eabp9435(2022).DOI:10.1126/sciadv.abp9435

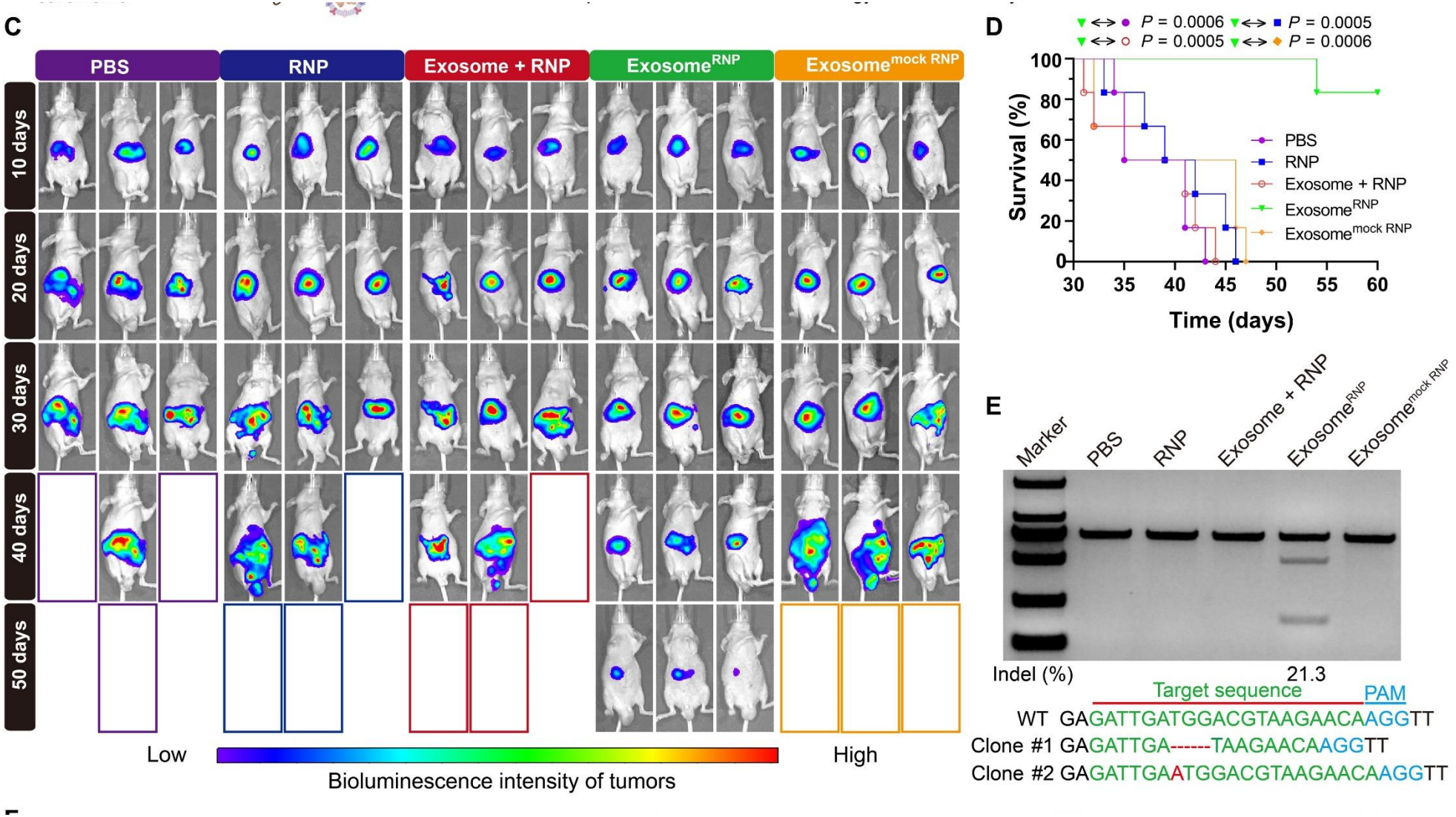

(**C**) In vivo luciferase expression of orthotopic HCC in the whole mice. (**D**) Survival rates after the specified treatments. Statistical significance was calculated by log-rank test (means ± SD, $n = 6$). (**E**) Frequency of indel mutation detected by T7E1 assay from liver tissues after the specified treatments.

*Sci. Adv.***8**,eabp9435(2022).DOI:10.1126/sciadv.abp9435

Lipid nanoparticles (LNPs) encapsulating Cas9 mRNA and sgRNA

CRISPR-LNP (cLNP) formulations containing Cas9 mRNA and an sgRNA were compared to Cas9 mRNA and sgRNAs encapsulated with the clinically approved LNP formulation, used for siRNA therapeutics, based on DLin-MC3-DMA as the ionizable cationic lipid (MC3-cLNPs).

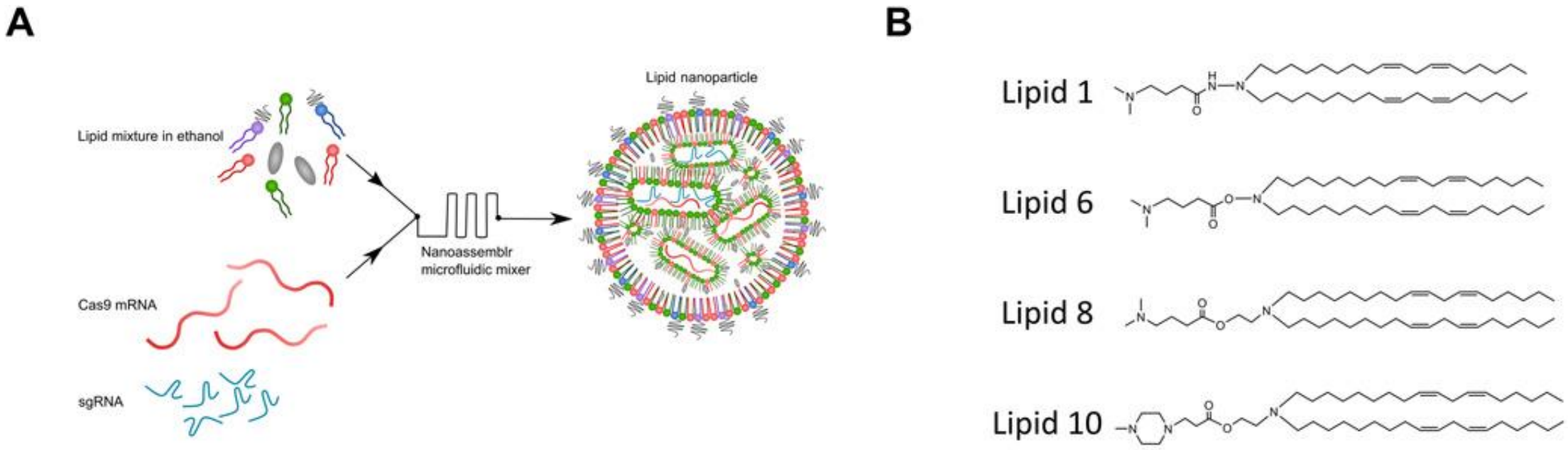

*Sci. Adv.***6**,eabc9450(2020).DOI:10.1126/sciadv.abc9450

To explore the potential of therapeutic genome editing, as proof of concept, we evaluated L8-cLNPs containing ***PLK1*** **sgRNA (sgPLK1-cLNPs)** or sgGFP-cLNPs as control. **PLK1 is a kinase required for mitosis**; lack of it leads to G_2-M phase cell cycle arrest and cell death in dividing cells.

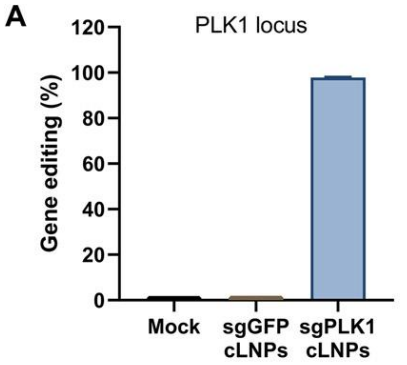

(**A**) Percentage of gene editing events (A) in the PLK1 loci as determined by NGS analysis (allelic frequencies of >2% are presented).

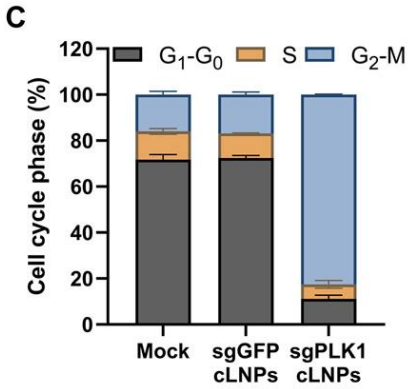

(**C**) Cell cycle analysis of HEK293 cells treated with mock, sgGFP, or sgPLK1-cLNPs (0.5 μg/ml, 3.5 nM of total RNA) for 48 hours and analyzed by flow cytometry. (C) Bar charts representing the percentage of G_1-S and G_2-M cell cycle phases.

(**E**) DAPI/annexin V assay of HEK293 cells treated with mock, sgGFP, or sgPLK1-cLNPs (0.5 μg/ml, 3.5 nM total RNA) for 96 hours and analyzed by flow cytometry. (E) Bar charts representing the percentage of live cells normalized to mock-treated cells.

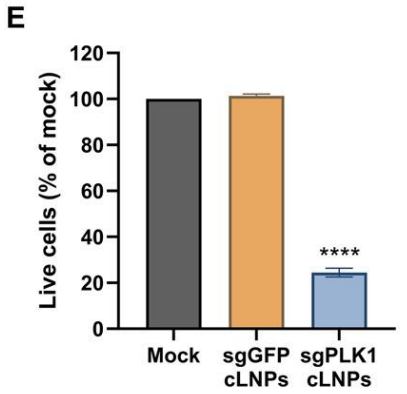

*Sci. Adv.***6**,eabc9450(2020).DOI:10.1126/sciadv.abc9450

These targeted LNPs are coated with cell-targeting antibodies by binding to a lipid-anchored single-chain antibody linker that recognizes the Fc region of rat immunoglobulin G2a [IgG2A; Anchored Secondary scFv Enabling Targeting (ASSET)] (Fig. 5A) and reduce the recognition of the targeting antibody by Fc receptors (*23*).

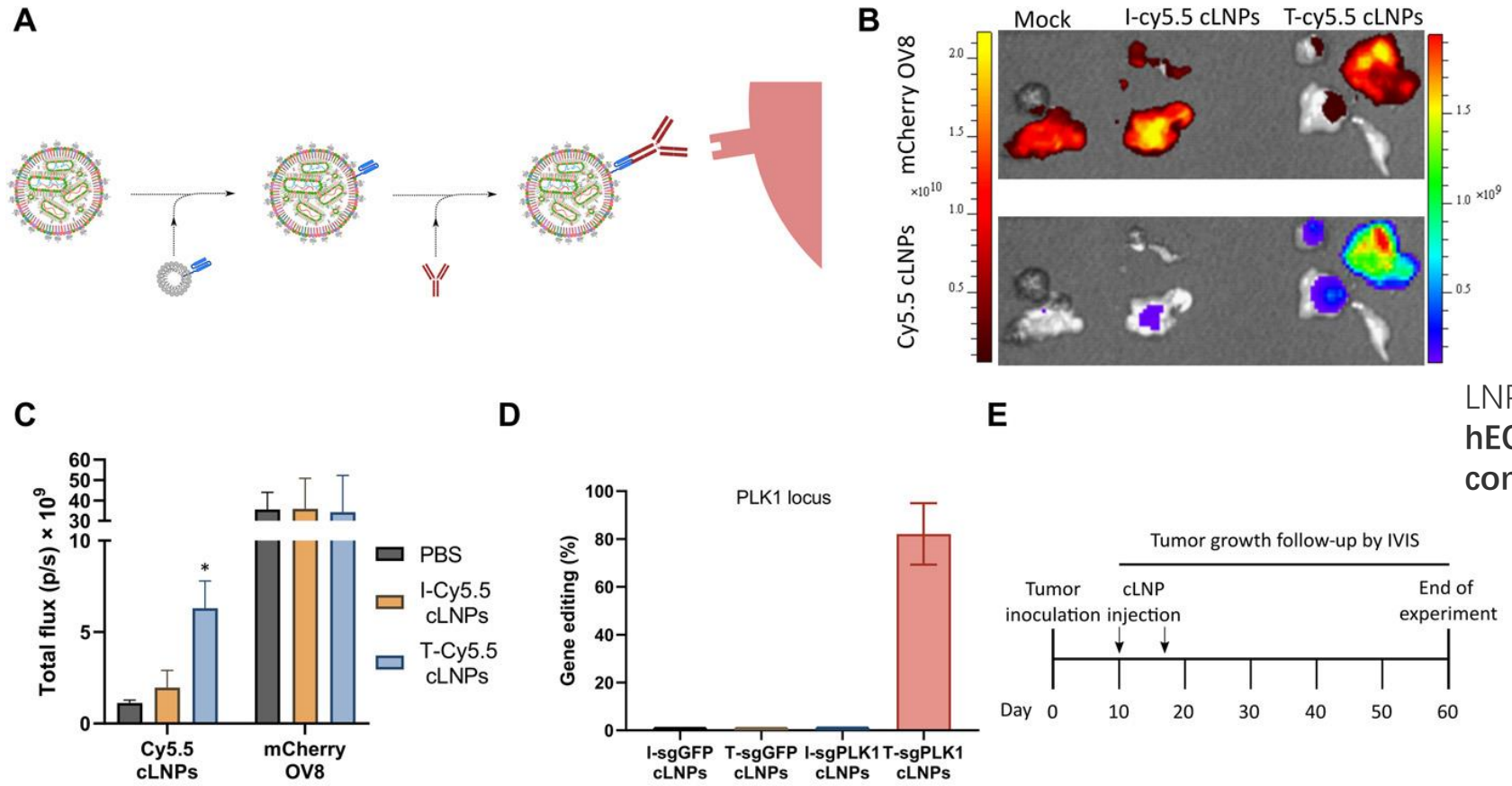

LNPs conjugated to **anti-hEGFR (T)** or **IgG isotype control (I)** antibody

(A) Schematic illustration of targeted cLNP production using ASSET (*23*).
(**B** and **C**) Tumor targeting and accumulation of Cy5.5-cLNPs in OV8 tumor–bearing mice as analyzed by the IVIS in vivo imaging system, 4 hours after injection. (B) Representative fluorescence imaging of tumors extracted from mCherry-OV8–bearing mice. Top, mCherry OV8 tumors; bottom, Cy5.5-cLNP signal accumulation.
(C) Quantification of mean fluorescence intensity of Cy5.5-cLNP accumulation in mCherry-OV8 tumors.
(**D**) Percentage of gene editing events in the PLK1 locus as determined by NGS analysis, 48 hours after injection of I-sgGFP, T-sgGFP, I-sgPLK1, or T-sgPLK1 cLNPs (0.75 mg/kg).

*Sci. Adv.***6**,eabc9450(2020).DOI:10.1126/sciadv.abc9450

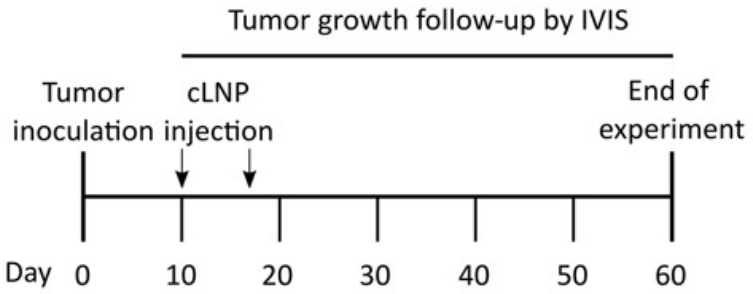

LNPs conjugated to **anti-hEGFR (T)** or **IgG isotype control (I)** antibody

(**E**) Experimental design. Ten and 17 days after tumor inoculation, I-sgGFP, T-sgGFP, I-sgPLK1, or T-sgPLK1 cLNPs (0.75 mg/kg) were injected intraperitoneally. Tumor growth was monitored using mCherry fluorescence of OV8-mCherry cells by the IVIS in vivo imaging system.

(**F** and **G**) Tumor growth inhibition by dual-dose treatment with cLNPs. (F) Representative fluorescence imaging of OV8-bearing mice. (G) OV8 tumor growth curve quantification.

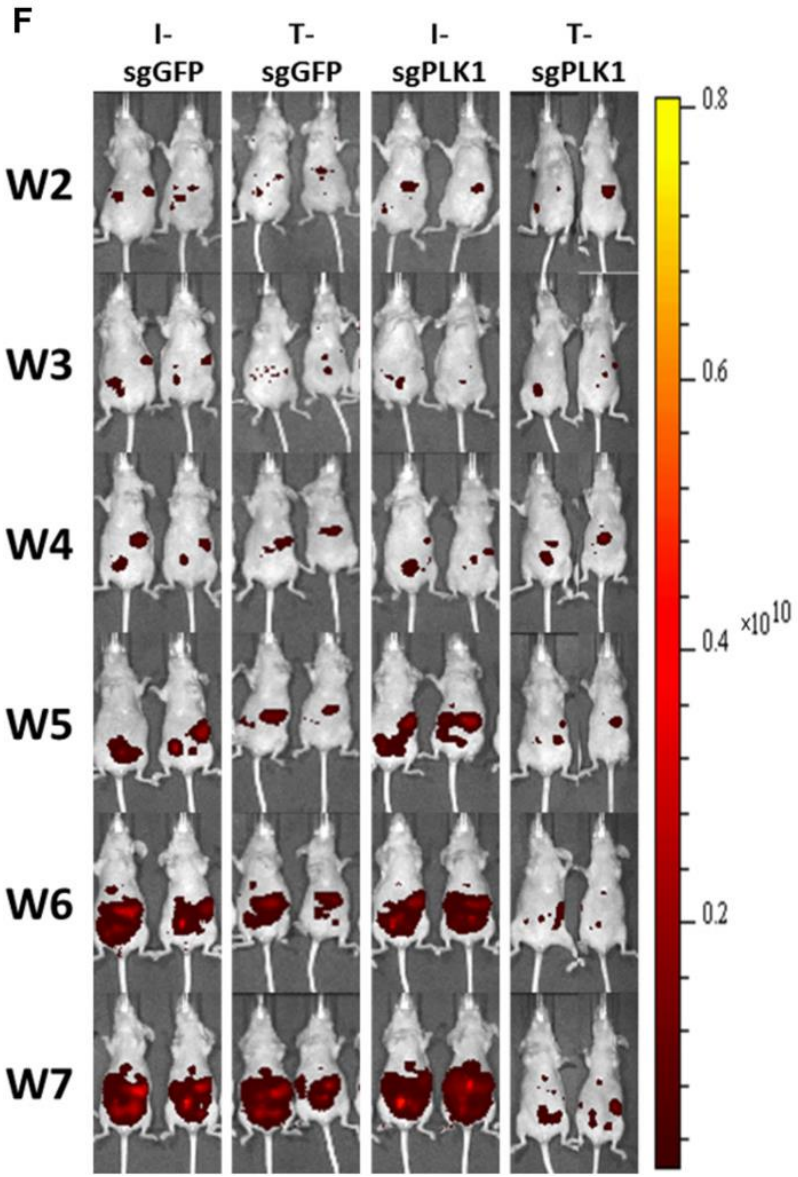

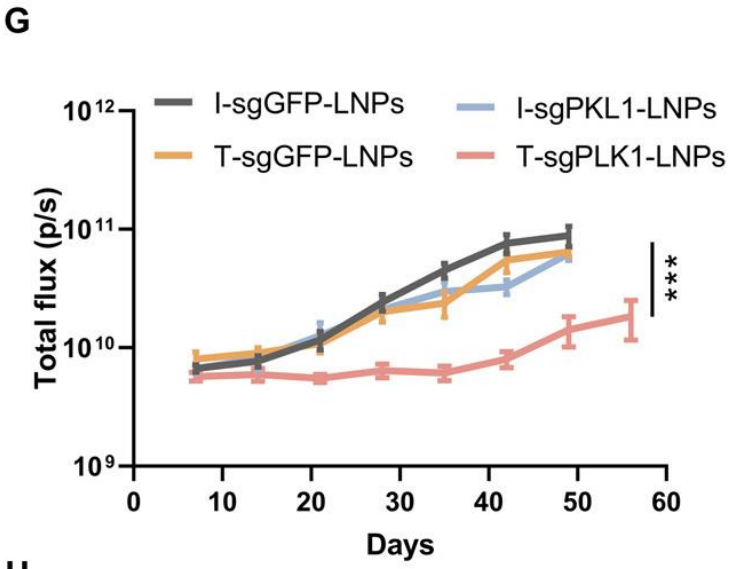

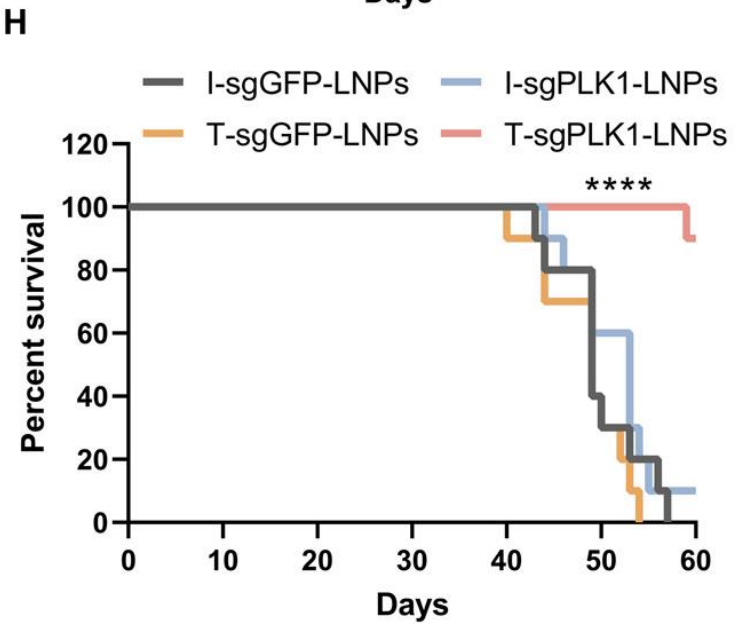

*Sci. Adv.***6**,eabc9450(2020).DOI:10.1126/sciadv.abc9450

Biomaterials to enhance cell therapy

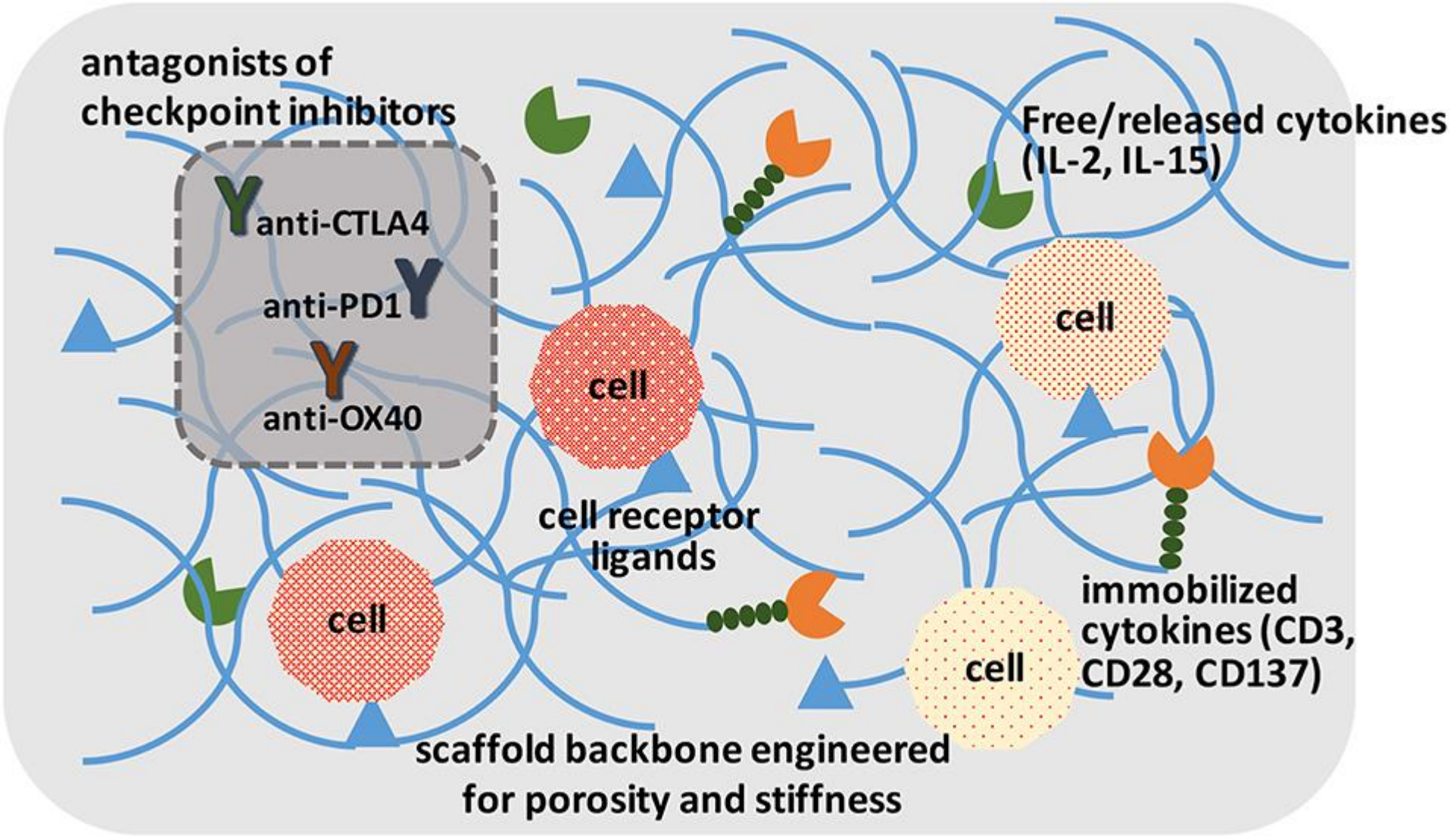

Genetic reprogramming using mRNA nanocarriers

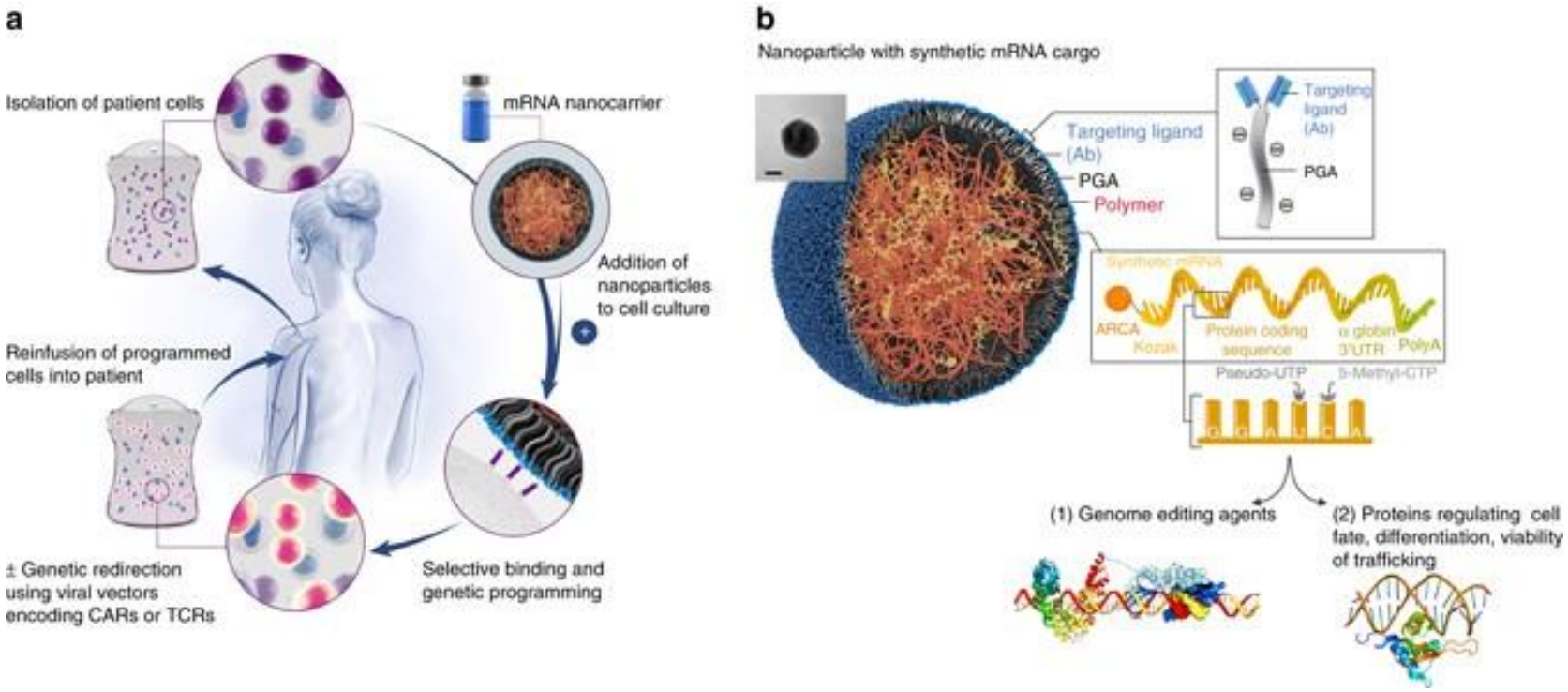

The viral and electroporation methods used to create adoptive cell therapies are complex and expensive. Consequently, we develop targeted mRNA nanocarriers that are simply mixed with cells to reprogram them via transient expression.

Nature Communications **volume 8**, Article number: 389 (2017)

$Foxo1_{3A}$-NP-transfection improves the anti-cancer activities of CAR T-cells.

NSG mice were inoculated with CD19 + Raji-luc tumor cells. After 7 days the mice were injected with luciferin and imaged on an IVIS before being randomly sorted into groups ($n = 9$) with representative tumor burden. Next 2.5×10^6 CD8+ 19-41BBζ CAR + T-cells (transfected with NPs loaded either with $Foxo1_{3A}$ mRNA or GFP mRNA) were infused intravenously.

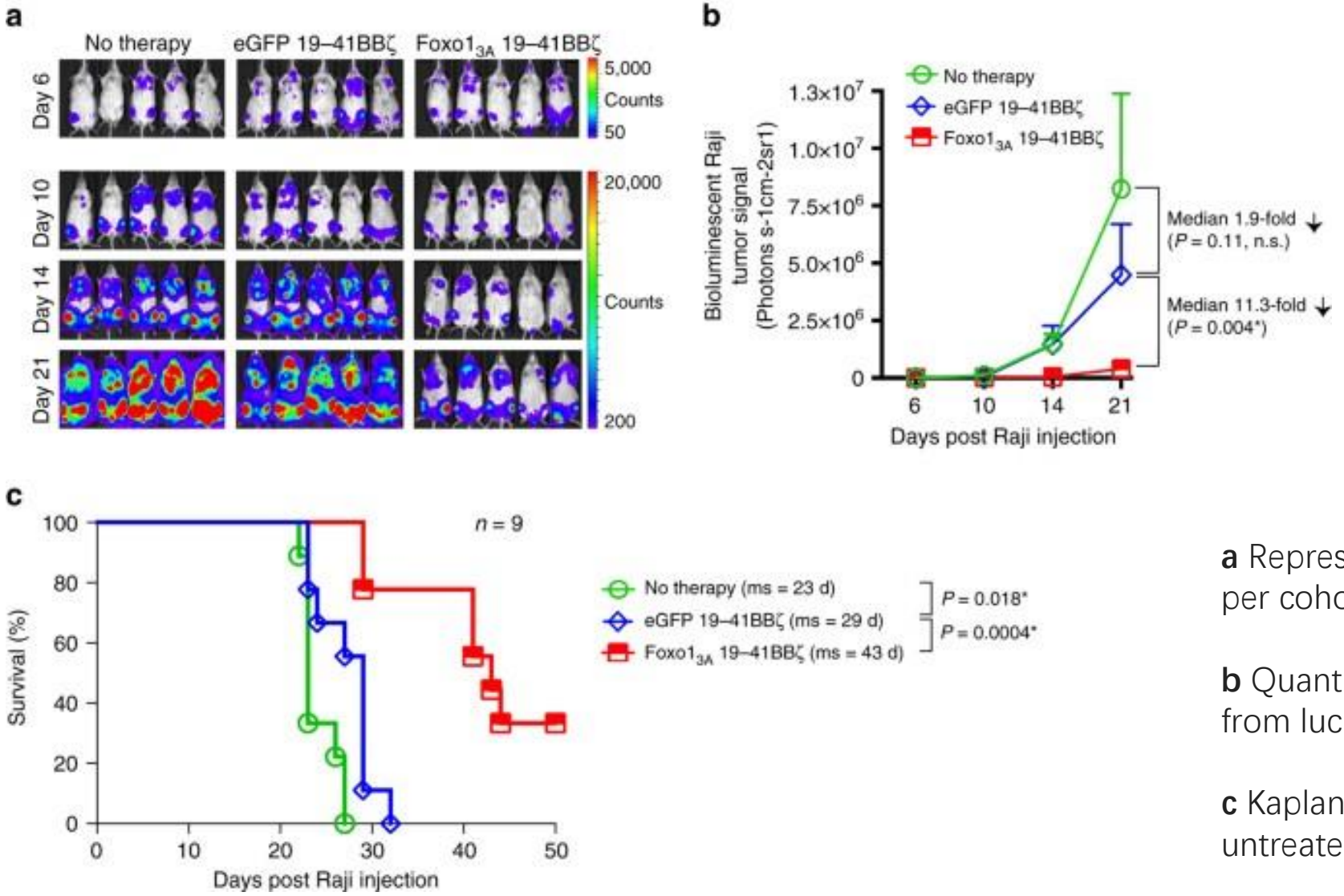

we transiently expressed **Foxo1** to reprogram the differentiation of effector cells into functionally competent memory cells

a Representative IVIS imaging depicting five mice per cohort.

b Quantified tumor burden (as mean radiance from luciferase activity from each mouse from **a**.

c Kaplan–Meier survival curves for treated and untreated control mice.

Nature Communications **volume 8**, Article number: 389 (2017)

Scaffolds expand primary T cells ex vivo

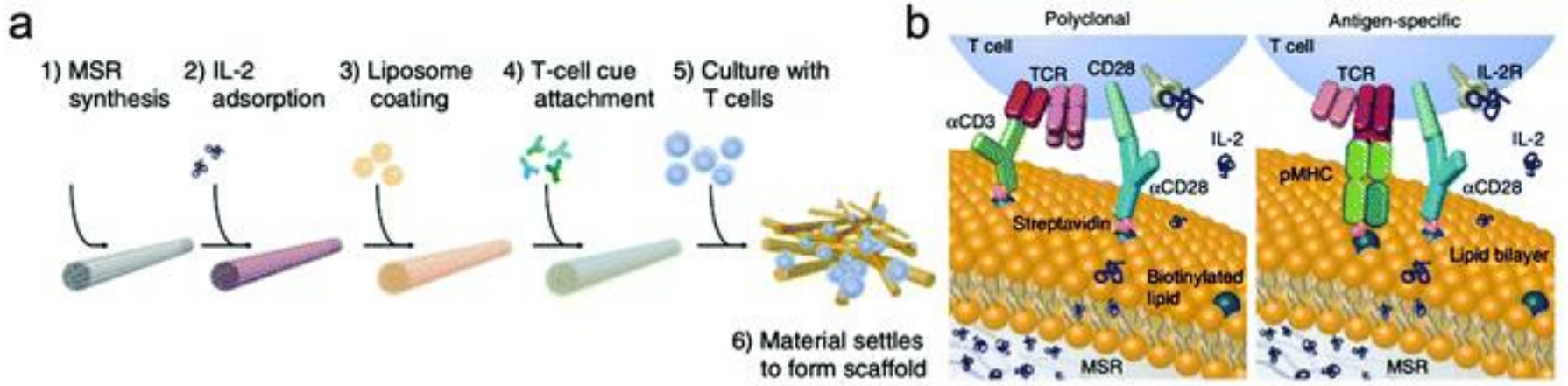

A mesoporous silica microrod (MSR) scaffold for multivalent T cell expansion.
(a) Scheme showing the synthesis process of an MSR-scaffold that mimics APCs.
(b) For polyclonal T-cell expansion, anti-CD3 and anti-CD28 activating antibodies are attached (left). For antigen-specific T-cell expansion, peptide-loaded MHC (pMHC) and anti-CD28 antibodies are attached (right).

Nature Biotechnology **volume 36**, pages160–169 (2018)

(c) Expansion of 19BBz T cells treated with Dynabeads or the MSR-scaffold.

(d) Normalized tumor growth kinetics (represented by quantified bioluminescent signals) of NSG mice treated with 19BBz T cells expanded for either 7 or 14 days with Dynabeads or the MSR-scaffold.

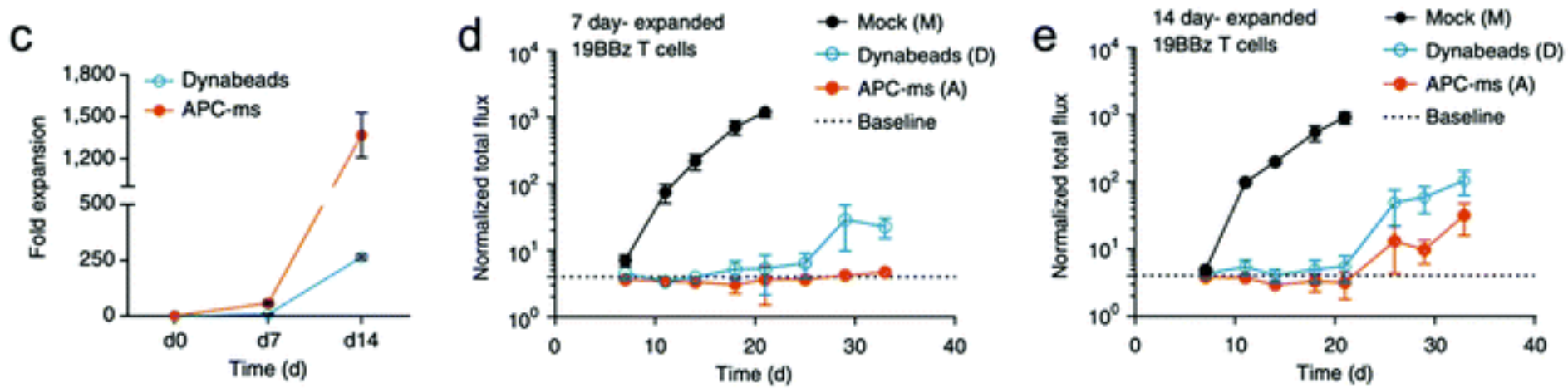

Hydrogel delivering CAR-T cells and anti-PDL1-conjugated platelets

A hyaluronic acid hydrogel for co-delivery of antigen-specific CAR-Ts and anti-PD-L1 antibody-conjugated platelets to prohibit post-surgery tumor recurrence.

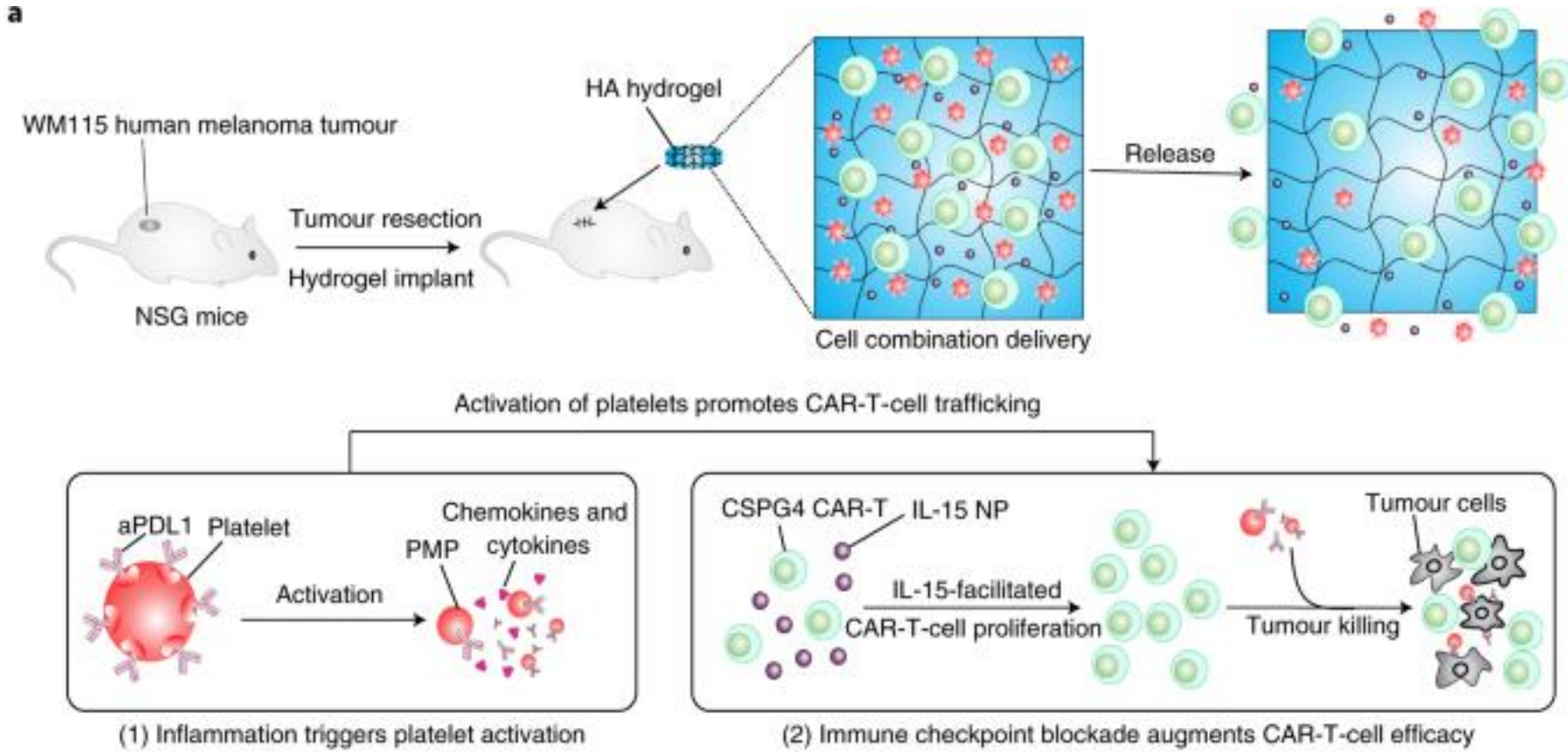

a, Schematic of the tumour resection model and implantation of the engineered HA hydrogel. Platelets activated during the wound healing process after surgery release aPDL1 in the form of PMP-aPDL1. MHC, major histocompatibility complex; TCR, T-cell receptor.

Nature Biomedical Engineering **volume 5**, pages1038–1047 (2021)

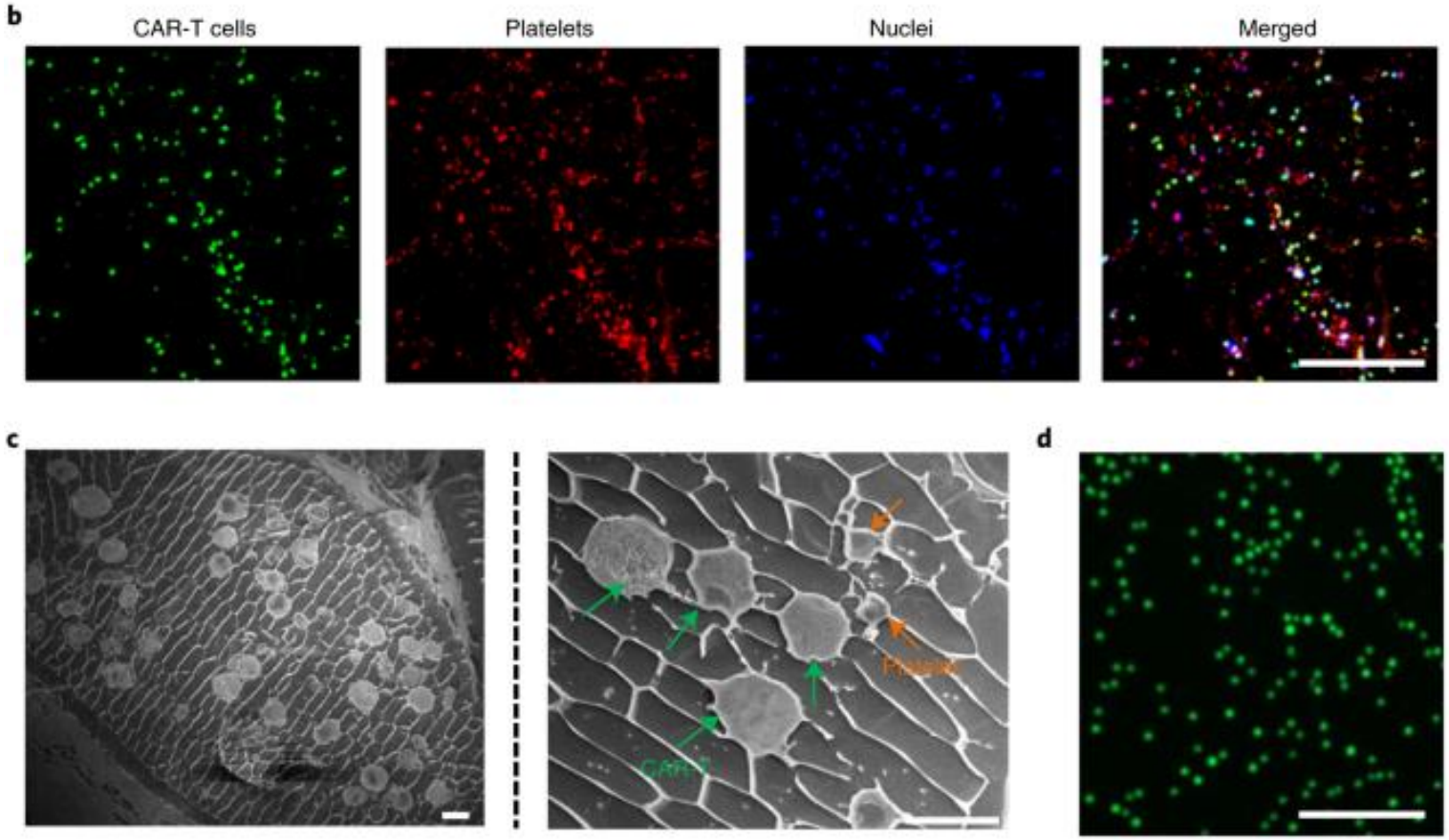

b, Confocal imaging of CAR-T cells and P–aPDL1 encapsulated in the hydrogel (CAR-T-P–aPDL1@gel). CAR-T cells and platelets were labelled with CellTracker Green and rhodamine B, respectively. Hoechst 33342 was used to stain the nuclei. Cell number, 2×10^6 CAR-T cells; platelet number, 1×10^7. This experiment was performed three times with similar results. Scale bar, 100 μm.

c, Cryo-scanning electron microscopy imaging of CAR-T-P–aPDL1@gel. Cell number, 2×10^6 CAR-T cells; platelet number, 1×10^7. Scale bars, 10 μm. This experiment was performed three times with similar results.

d, Confocal imaging of the live/dead assay of CAR-T cells released from the hydrogel. Live cells and dead cells were labelled with green fluorescence and red fluorescence, respectively. Scale bar, 100 μm. This experiment was performed three times with similar results.

Nature Biomedical Engineering **volume 5**, pages1038–1047 (2021)

CAR-T cells encapsulated in the hydrogel control WM115 melanoma growth in vivo.

a, Representative tumour bioluminescence. P–aPDL1@gel, P–aPDL1 encapsulated in the hydrogel; CAR-T, CAR-T cells directly inoculated into the resection cavity; CAR-T + P–aPDL1, CAR-T cells and aPDL1 directly inoculated into the resection cavity; CAR-T@gel, CAR-T cells encapsulated in the hydrogel; CAR-T@gel + P–aPDL1, CAR-T cells encapsulated in the hydrogel and P–aPDL1; CAR-T-P–aPDL1@gel, CAR-T cells and P–aPDL1 co-encapsulated in the hydrogel. In all of the experimental groups, IL-15 NPs (IL-15, 1 μg) were included. Cell number, 2×10^6 CAR-T cells; platelet number, 1×10^7. The amounts of aPDL1 and IL-15 were both 1 μg.

b, Region-of-interest analysis of tumour bioluminescence intensities.

c, Comparison of tumour bioluminescence intensities at week 3 after treatment.

d, Summary of the tumour volume at week 3 after treatment.

e, Representative tumours after 3 weeks. Scale bar, 1 cm.

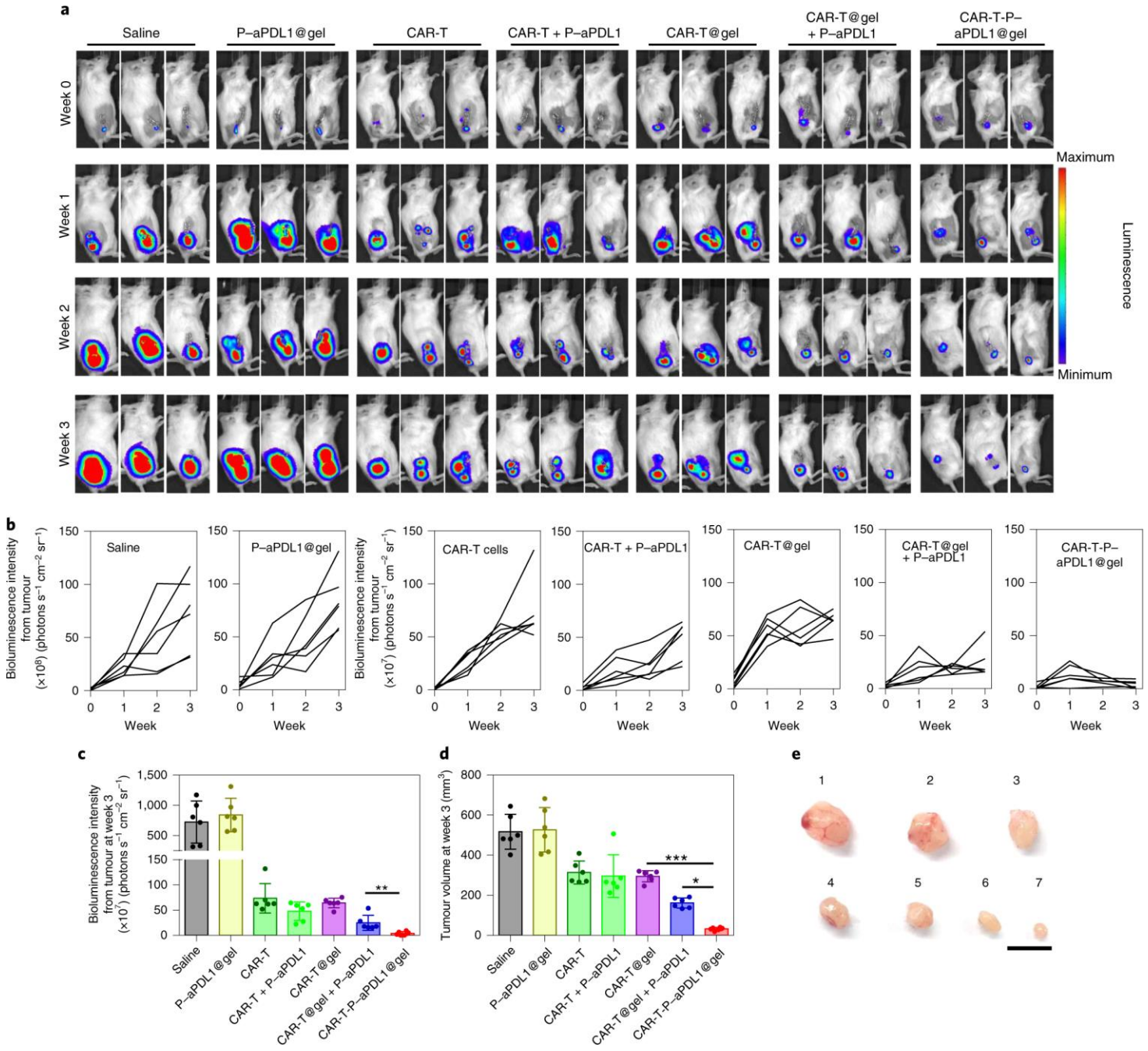

Nature Biomedical Engineering **volume 5**, pages1038–1047 (2021)